London
Journals Press

IMAGE: OBSERVATORY WITH STAR TRAILS ON MOUNTAINS FOR CLEAR SKY

London Journals Press

They were leaders in building the early foundation of modern programming and unveiled the structure of DNA Their work inspired environmental movements and led to the discovery of new genes They've gone to space and back taught us about the natural world dug up the earth and discovered the origins of our species They broke the sound barrier and gender barriers along the way The world of research wouldn't be the same without the pioneering efforts of famous research works made by these women Be inspired by these explorers and early adopters- the women in research who helped to shape our society We invite you to sit with their stories and enter new areas of understanding This list is by no means a complete record of women to whom we are indebted for their research work but here are of history's greatest research contributions made by...

Read complete here:
https://goo.gl/1vQ3lS

Women In Research

Computing in the cloud!

Cloud Computing is computing as a Service and not just as a Product Under Cloud Computing...

Read complete here:
https://goo.gl/VvHC72

Writing great research...

Prepare yourself before you start Before you start writing your paper or you start reading other...

Read complete here:
https://goo.gl/np73jP

Journal Content
In this Issue

London
Journals Press

Editorial Board

Curated board members

Dr. Saad Subair

College of Computer and Information Sciences, Alazaeim Alazhari University, Khartoum North, Sudan, Associate Professor of Computer Science and Information Ph.D., Computer Science Bioinformatics, University of Technology Malasiya

Gerhard X Ritter

Emeritus Professor, Department of Mathematics, Dept. of Computer & Information, Science & Engineering Ph.D., University of Wisconsin-Madison, USA

Dr. Ikvinderpal Singh

Assistant Professor, P.G. Deptt. of Computer Science & Applications, Trai Shatabdi GGS Khalsa College, India

Prof. Sergey A. Lupin

National Research, University of Electronic Technology Ph.D., National Research University of Electronic Technology, Russia

Dr. Sharif H. Zein

School of Engineering, Faculty of Science and Engineering, University of Hull, UK Ph.D., Chemical Engineering Universiti Sains Malaysia, Malaysia

Prof. Hamdaoui Oualid

University of Annaba, Algeria Ph.D., Environmental Engineering, University of Annaba, University of Savoie, France

Prof. Wen Qin

Department of Mechanical Engineering, Research Associate, University of Saskatchewan, Canada Ph.D., Materials Science, Central South University, China

Luisa Molari

Professor of Structural Mechanics Architecture, University of Bologna, Department of Civil Engineering, Chemical, Environmental and Materials, PhD in Structural Mechanics, University of Bologna.

Prof. Chi-Min Shu

National Yunlin University of Science and Technology, Chinese Taipei Ph.D., Department of Chemical Engineering University of Missouri-Rolla (UMR) USA

Prof. Te-Hua Fang

Department of Mechanical Engineering, National Kaohsiung University of Applied Sciences, Chinese Taipei Ph.D., Department of Mechanical Engineering, National Cheng Kung University, Chinese Taipei

Dr. Fawad Inam

Faculty of Engineering and Environment,
Director of Mechanical Engineering,
Northumbria University, Newcastle upon Tyne,
UK, Ph.D., Queen Mary, University of London,
London, UK

Dr. Rocío Maceiras

Associate Professor for Integrated Science,
Defense University Center, Spain Ph.D., Chemical
Engineering, University of Vigo, SPAIN

Muhammad Hassan Raza

Postdoctoral Fellow, Department of Engineering
Mathematics and Internetworking,
Ph.D. in Internetworking Engineering,
Dalhousie University, Halifax Nova Scotia,
Canada

Rolando Salgado Estrada

Assistant Professor,
Faculty of Engineering, Campus of Veracruz,
Civil Engineering Department, Ph D.,
Degree, University of Minho, Portugal

Abbas Moustafa

Department of Civil Engineering,
Associate Professor, Minia University, Egypt, Ph.D
Earthquake Engineering and Structural Safety,
Indian Institute of Science

Dr. Babar shah

Ph.D., Wireless and Mobile Networks,
Department of Informatics,
Gyeongsang National University,
South Korea

Dr. Wael Salah

Faculty of Engineering,
Multimedia University Jalan Multimedia,
Cyberjaya, Selangor, Malaysia, Ph.D, Electrical and
Electronic Engineering, Power Electronics
and Devices, University Sians Malaysia

Prof. Baoping Cai

Associate Professor,
China University of Petroleum,
Ph.D Mechanical and Electronic Engineering,
China

Prof. Zengchang Qin

Beijing University of Aeronautics
and Astronautics Ph.D.,
University of Bristol,
United Kingdom

Dr. Manolis Vavalis

University of Thessaly,
Associate Professor, Ph.D.,
Numerical Analysis,
University of Thessaloniki, Greece

Dr. Mohammad Reza Shadnam

Canadian Scientific Research and Experimental
Development Manager-Science,
KPMG LLP, Canada, Ph.D., Nanotechnology,
University of Alberta, Canada

Dr. Gang Wang

HeFei University of Technology,
HeFei, China, Ph.D.,
FuDan University, China

Kao-Shing Hwang

Electrical Engineering Dept.,
Nationalsun-Yat-sen University Ph.D.,
Electrical Engineering and Computer Science,
Taiwan

Mu-Chun Su

Electronics Engineering,
National Chiao Tung University, Taiwan,
Ph.D. Degrees in Electrical Engineering,
University of Maryland, College Park

Zoran Gajic

Department of Electrical Engineering,
Rutgers University, New Jersey, USA
Ph.D. Degrees Control Systems,
Rutgers University, United States

Dr. Homero Toral Cruz

Telecommunications,
University of Quintana Roo, Ph.D.,
Telecommunications Center for Research
and Advanced Studies National Polytechnic
Institute, Mexico

Nagy I. Elkalashy

Electrical Engineering Department,
Faculty of Engineering,
Minoufiya University, Egypt

Vitoantonio Bevilacqua

Department of Electrical and Information
Engineering Ph.D., Electrical Engineering
Polytechnic of Bari, Italy

Dr. Sudarshan R. Nelatury

Pennsylvania State University USA Ph.D., Signal
Processing Department of Electronics and
Communications Engineering,
Osmania University, India

Prof. Qingjun Liu

Professor, Zhejiang University, Ph.D.,
Biomedical Engineering,
Zhejiang University, China

Sanjukta Pookulangara

College of Merchandising,
Hospitality and Tourism,
University of North Texas, USA Ph.D, Fashion
Merchandising, University of Missouri Columbia

Prof. Yaohua Zhu

Hong Kong Polytechnic University,
China, PhD. Applied Science and Engineering,
 Metallurgy and Materials,
Aston University, UK

Jeng-Da Chai

Associate Professor, Department of Physics,
National Taiwan University,
Excellent Junior Research Investigators,
Ministry of Science and Technology,
Career Development Award,
National Taiwan University

Prof. Peter K. Law

Huazhong University of Science and Technology,
Ph.D., University of Toronto B.Sc.,
McGILL University

Yas Al-Sultani

Ph.D. Image processing Enhancement
using Fuzzy Set Theory Arabian Gulf University,
Constituencies, Training and Continuous
Teaching Center, Iraq

Prof. Dimitrios A. Papaconstantopoulos

School of Physics, Astronomy, and Computational
Sciences, George Mason University, USA
Ph.D., Theoretical Solid State Physics
University of London(UK)

Dr. Abdelkader Zarrouk

Faculty of Sciences, Dept. of Chemistry
Laboratory Applied Chemistry and Environment
Mohammed First University Ph.D.,
Mohammed First Unversity Oujda, Morocco

Prof. Tai-Yin Huang

Associate Professor of Physics, Pennsylvania
State University, Penn State Lehigh Valley,
Ph.D., Physics, University of Cincinnati,
President of the Lehigh Valley,
 Taiwanese Women Association

Prof. Dr. Ahmed Asaad Ibrahim Khalil

National Institute for Laser Enhanced Sciences,
NILES Cairo University, Giza, Egypt Ph.D.,
Experimental Physics V Institute
Engineering Application of Lasers
University Bochum, Germany

Dr. Mohamed Salem Badawi

Department of Physics,
Awarded Junior Radiation Physics Medal,
7th Radiation Physics and Protection
Conference, Ismailia, Egypt

Prof. Marie-Christine Record

Department of Chemistry,
Aix-Marseille University Ph.D.,
Materials Sciences, Montpellier University,
France

Prof. Hakan Arslan

Mersin University Ph.D.,
Chemistry Nigde University
Turkey

Prof. Wanyang Dai

Department of Mathematics,
Nanjing University, China
Ph.D., Applied Mathematics,
Georgia Institute of Technology, USA

Dr. Hyongki Lee

Assistant Professor,
University of Houston
Ph.D. in Geodetic Science,
Ohio State University, USA

Nicola Mastronardi

Consiglio Nazionale delle Ricerche,
Ph.D. Applied Mathematics Katholieke
Universiteit Leuven
Belgium

Prof. Saad Belkhiat

Setif University, Ph.D., Physics
University of Sétif
Algeria

Dr. Arvind Chhabra

University of Connecticut Health Center
USA Ph.D., Biotechnology Central
Drug Research Institute

Mohamed Shaaban Ali

Department of Anaesthetics,
Al Salam International Hospital,
The State of Kuwait PhD,
Cerebral Monitoring during cardiac surgery,
University of Wales, Cardiff, UK

Prof. Tarek Aboul-Fadl Mohammad Hassan

Vice Dean for Education and Student Affairs,
Department of Medicinal Chemistry,
Faculty of Pharmacy, Assiut University

Prof. Anthony Bridgwater

European Bioenergy Research Institute,
Director of EBRI, Leader of Aston University
Bioenergy Research Group,
Edwin Walker Prize winner

Prof. Ewa Szczepanska-Sadowska

Medical University of Warsaw,
Poland Ph.D., Medical University of Warsaw,
Poland

Prof. Gjumrakch Aliev

University of Atlanta, Ph.D.,
Cardiovascular Biology and Pathology,
Moscow State University

Prof. Elsayed Ibrahim ELAGAMY

Department of Applied Medical Sciences,
Qassim University, Kingdom of Saudi Arabia,
Ph.D., Dept. of Comparative Medicine,
Mc Gill University

Shen Hu

Division of Oral Biology and Medicine,
Jonsson Comprehensive Cancer Center,
University of California, Ph.D.,
Bioanalytical Chemistry, Wuhan University,
China

Rahul Mahavir Nandre

College of Veterinary Medicine,
Kansas State University, Kansas, USA Ph.D.,
Veterinary Medicine Chonbuk National University,
South Korea

A. C. Matin

Department of Microbiology and Immunology,
Stanford University School of Medicine Stanford,
California Ph.D., Microbiology,
University of California, Los Angeles

Wei Wang

Professor, Public Health School of
Medical Sciences, Ph.D., Edith Cowan University,
Australia

Prof. Filippo Berto

Department of Management and Engineering,
University of Padua, Italy
PH.D, University of Florence

Prof. Bernardino Benito

Department of Accounting and Finance,
Faculty of Economics and Business,
Ph.D. in Economics and Business,
University of Murcia, SPAIN

Dr. Dimitrios Vortelinos

Department of Accounting,
Economics and Finance, University of Lincoln,
UK Ph.D., Financial Economics,
University of Peloponnese, Greece

Victor J. Tremblay

Department of Economics,
Oregon State University Ph.D.,
Economics Washington State University

Dr. Emmily Mugasia

Department of Education planning and
Management, Masinde Muliro University of Science
and Technology Kakamega – Kenya.

Dr. Randall Xu

School of Business,
Accounting Department University of Houston
-Clear Lake Ph.D. Accounting University of Alabama

Prof. Bartlomiej Kaminski

Information Technology and Management Rzeszow
University Poland Ph.D., Department of Economics
University of Warsaw, Poland

Prof. Ubaldo Comite

University of Calabria,
Arcavacata – Rende,
Italy University Giustino Fortunato,
Benevento – Italy Ph.D.,
Economy and Management
of Public Administrations

Prof. Birendra (Barry) Mishra

Professor of Accounting
A. Gary Anderson Graduate School of Management
University of California, Riverside,
USA Ph.D., Accounting University of Texas, Austin

Xuebing Yang

Assistant Professor,
Economics Penn State Altoona Ph.D.,
University of Oklahoma USA

Prof. Robin H. Luo

Professor of Finance ALHOSN University, UAE
Adjunct DBA Faculty Doctoral Supervisor
University of Liverpool/Laureate, UK Ph.D.,
Nanyang Technological University
Singapore

Omonijo Ojo

Student Industrial Work Experience
Scheme Covenant University, Ota,
Ogun-State Obafemi Awolowo
University Sociology of Development Covenant
University, University Ota, Nigeria

Dr. Haijing Dai

Assistant Professor Chinese University of
Hong Kong Department of Social Work Doctor of
Philosophy Social Work and Sociology University of
Michigan, Ann Arbor

Prof. Yung C. Shin

Purdue University,
USA Ph.D.,
University of Wisconsin, USA

Dr. Xiaochun Cheng

Middlesex University,
UK Ph.D.,
Jilin University China

Prof. Tatiana Kovacikova

COST Office Belgium Ph.D.,
University of Zilina
Slovakia

Dr. José Reinaldo Silva

University of São Paulo Ph.D.,
University of São Paulo
Brazil

Prof. Chang-Hwan Lee

Dong Guk University,
South Korea Ph.D.,
University of Connecticut USA

Prof. Qiuqi Ruan

Beijing Jiaotong University B.S.,
Northern Jiaotong University Beijing

Prof. Victor J. Tremblay

Oregon State University Ph.D.,
Washington State University,
University of California
USA

Prof. Vassili Kolokoltsov

University of Warwick,
UK Ph.D., Moscow State University,
Russia

Development of Novel Kinetic Energy Functional for Orbital-Free Density Functional Theory Applications-II

Vittoria Urso

"Marconi" Building University City of Rome - Sapienza

ABSTRACT

The development of novel Kinetic Energy (KE) functionals is an important topic in density functional theory (DFT). Here, I present a study of Laplacian-Level kinetic energy functionals applied to metallic nanosystems. The nanoparticles are modeled using jellium spheres of different sizes, background densities, and number of electrons. The ability of different functionals to reproduce the correct kinetic energy density and potential of various nanoparticles is investigated and analyzed in terms of semilocal descriptors. Most semilocal KE functionals are based on modifications of the second-order gradient expansion GE2 or GE4. After a series of calculations and analyzes on the second and fourth order gradient expansion and respecting the exact constraints, I propose a new functional LAP1 which allows to remove the divergence of the potential of the functional GE4 and to obtain lower errors of both energy and potential.

Keywords: DFT, kinetic energy functional, jellium spheres.

Classification: DDC Code: 530.41 LCC Code: QC176.8.E4

Language: English

Development of Novel Kinetic Energy Functional for Orbital-Free Density Functional Theory Applications-II

Vittoria Urso

ABSTRACT

The development of novel Kinetic Energy (KE) functionals is an important topic in density functional theory (DFT). Here, I present a study of Laplacian-Level kinetic energy functionals applied to metallic nanosystems. The nanoparticles are modeled using jellium spheres of different sizes, background densities, and number of electrons. The ability of different functionals to reproduce the correct kinetic energy density and potential of various nanoparticles is investigated and analyzed in terms of semilocal descriptors. Most semilocal KE functionals are based on modifications of the second-order gradient expansion GE2 or GE4. After a series of calculations and analyzes on the second and fourth order gradient expansion and respecting the exact constraints, I propose a new functional LAP1 which allows to remove the divergence of the potential of the functional GE4 and to obtain lower errors of both energy and potential.

Keywords: DFT, kinetic energy functional, jellium spheres.

Author: Department of Physics - "Marconi" Building University City of Rome - Sapienza, Piazzale Aldo Moro, 2, 00185 Rome RM, Italy.

I. INTRODUCTION

Density functional theory (DFT) is one of the most widely used approaches for theoretical calculations in solid-state physics and quantum chemistry[1]. In its original orbital-free (OF) formulation[2,3], DFT allows one to describe the ground state of a many-electron system[4] as a function of the electron density (ρ) alone, through the solution of the Euler equation[5]:

$$\frac{\delta T_s[\rho]}{\delta\rho(\mathbf{r})} + \nu_{ext}(\mathbf{r}) + \nu_J(\mathbf{r}; [\rho]) + \frac{\delta E_{xc}[\rho]}{\delta\rho(\mathbf{r})} = \mu \qquad (1)$$

where $T_s[\rho]$ is the noninteracting kinetic energy (KE) density functional; $\nu_{ext}(\mathbf{r})$ and $\nu_J(\mathbf{r}; [\rho])$ are the external (i.e. nuclear) and Coulomb potentials, respectively; $E_{xc}[\rho]$ is the exchange correlation (XC) energy functional; and the Lagrange multiplier μ is the chemical potential, which takes into account that the number of electrons is fixed. Equation (1) is of limited practical utility, since only $\nu_J(\mathbf{r}; [\rho])$ is known its exact functional form, while $T_s[\rho]$ and $E_{xc}[\rho]$ are not known as explicit functionals of electron density. For the term XC, many different useful approximations have been developed for different types of systems (molecules, solids, surfaces, atoms, etc.) considering the fact that Exc [] is by far the smallest term in Eq. (1). For the functional non-interacting kinetic energy, there are still no reliable approximations. DFT it is conventionally implemented in the Kohn-Sham[6] scheme by introducing an auxiliary set of non-interacting particles to describe the density of the ground state. Alternative methods are: i) Free Orbital DFT (OF-DFT) methods, including the hydrodynamic model to describe the absorption spectra of nanoparticles[7] ; ii) Embedding methods (e.g. subsystem[8] DFT, partition[9] DFT), in-

cluded their linear response extensions[10]. These methods consist in dividing the main system in smaller interacting fragments, allowing a reduced computational cost.

All of these methods have in common that they need an explicit density functional expression for the kinetic energy (KE) of electrons, including the first e second functional derivative, i.e. the kinetic potential and the kinetic kernel, respectively. The exact explicit form of the $T_s[\rho]$, as a functional of the electron density, is known only for

- the homogeneous electron gas (HEG), i.e., the Thomas-Fermi (TF) local functional[5,11]

$$T_s^{TF}[\rho] = \int \tau^{TF}(\mathbf{r})d\mathbf{r} = \int C_{TF}\rho^{5/3}(\mathbf{r})d\mathbf{r} \qquad (2)$$

  with $C_{TF} = 3/10(3\pi^2)^{2/3} \simeq 2.8712$, the TF constant.

- 1 and 2 electron systems, i.e., the von Weizsacker (VW) functional

$$T_s^{VW}[\rho] = \int \tau^{VW}(\mathbf{r})d\mathbf{r} = \int \frac{|\nabla\rho(\mathbf{r})|^2}{8\rho(\mathbf{r})}d\mathbf{r} \qquad (3)$$

The same holds for the kinetic kernel. In between these two extreme cases, different semilocal or nonlocal approximations were developed in recent years. Non-local KE functionals are rather accurate, but they are derived mainly from the linear response of the homogeneous electron gas (the Lindhard function[12]) and are thus only suitable for solid-state simulations. Semilocal KE functionals are instead usually developed on the basis of the generalized gradient expansion or its resummation.

London Journal of Research in Science: Natural and Formal

The approximation (2) is not very accurate for real applications but it is the basis to construct generalized gradient approximations (GGAs)[13–16]:

$$T_s^{GGA}[\rho] = \int \tau^{TF} F_s(s(\mathbf{r})) \, d\mathbf{r} \qquad (4)$$

where F_s, called *enhancement factor*, is an appropriate function of the *reduced gradient*:

$$s = \frac{|\nabla \rho|}{2(3\pi^2)^{1/3}\rho^{4/3}} \qquad (5)$$

and therefore for $F_s = 1$ I obtain the TF (Thomas-Fermi) KE functional. The GGAs are the most popular KE approximations also known as semilocal. The functional (3) is a lower bound for the kinetic energy and is accurate in nuclear and asymptotic regions, its enhacement factor is:

$$F_s = \frac{5}{3}s^2 \qquad (6)$$

Gradient expansions are poweful theoretical tools which describe with accuracy the KE slowly varying density regime of an electronic system, providing an ideal starting point for the development of approximate KE models. One model is obtained including a new ingredient in the kinetic enhancement factor[17,18]: the laplacian of the density yielding the class of Laplacian-Level meta-GGAs (LL-meta-GGAs)[19]

$$T_s^{LL}[\rho] = \int \tau^{TF} F_s(\rho, \nabla\rho, \nabla^2\rho) \, d\mathbf{r} \qquad (7)$$

Under a uniform scaling of the density

$$\rho_\lambda(\mathbf{r}) = \lambda^3 \rho(\lambda \mathbf{r}), \quad \lambda \geq 0 \qquad (8)$$

the exact non-interacting kinetic energy behaves as

$$T_s[\rho_\lambda] = \lambda^2 T_s[\rho] \qquad (9)$$

i.e. as the Thomas-Fermi KE. Therefore, to have eq.(7) satisfy this constraint, $F_s(\rho, \nabla\rho, \nabla^2\rho, ...)$ must be invariant under the uniform density scaling. Such a goal can be achieved by considering the following dimensionless reduced gradient and laplacian

$$p = \frac{|\nabla\rho|^2}{4(3\pi^2)^{2/3}\rho^{8/3}} \quad , \quad q = \frac{\nabla^2\rho}{4(3\pi^2)^{2/3}\rho^{5/3}} \qquad (10)$$

The enhancement factor becomes therefore

$$F_s(\rho, \nabla\rho, \nabla^2\rho) = F_s(p, q) \qquad (11)$$

II.   THEORY

The Thomas-Fermi (TF) model makes the origin of DFT. The TF model is only exact for the free-electron gas (FEG). Calculations with this model didn't explain the exchange-correlation effects and the kinetic-energy density functional. Using the approximation for realistic systems yields poor quantitative predictions, even failing to reproduce some general features of the density such as shell structure in atoms and Friedel oscillations in solids. It has, however, found modern applications in many fields through the ability to extract qualitative trends analytically and with the ease at which the model can be solved. The kinetic energy expression of Thomas-Fermi theory is also used as a component in more sophisticated density approximation to the kinetic energy within modern orbital-free density functional theory[18].

Can be calculated the kinetic energy and the kinetic potential of the systems with the 41 kinetic functionals that can be found in Libxc[20], 2 LDA (Local Density Approximation) and 39 GGA (Generalized Gradient Approximation). Libxc is a library of exchange-correlation functionals for density functional theory. In Libxc it can find different types of functionals: LDA, GGA, hydrids, and mGGA. These functionals depend on local information, in the sense that the value of the potential at a given point depends only on the values of the density and the gradient of the density and the kinetic energy density.

In the following there are some of the enhancement factor of the 41 kinetic functionals with particular relevance for the present work:

• 1. LDA, Thomas-Fermi

$$F_s^{TF} = 1 \qquad (12)$$

• 3. GGA, Thomas-Fermi plus von Weiszaecker correction

$$F_s^{TF} = 1 + \frac{5}{3}s^2 \qquad (13)$$

• 4-8. GGA, PBE-like

$$F_s^{PBEn} = 1 + \sum_1^{n-1} C_i^{(n)} \left(\frac{s^2}{1+a^{(n)}} s^2 \right)^i \qquad (14)$$

• 11. GGA, Tran and Wesolowski TW02

$$F_s^{TW02} = 1 + \kappa - \frac{\kappa}{1 + \frac{\mu}{\kappa}s^2} \qquad (15)$$

where $\kappa = 0.8438$ and $\mu = 0.2319$.

• 13. GGA, von Weiszaecker corretion to Thomas-Fermi

$$F_s^{vW} = \frac{5}{3}s^2 \qquad (16)$$

• 14. GGA, second-order gradient expansion

$$F_s^{GE2} = 1 + \frac{5}{27}s^2 \qquad (17)$$

- 15-18. GGA, TFλvW

$$F_s^{TF} = 1 + \lambda \frac{5}{3} s^2 \qquad (18)$$

- 25. GGA, Ou-Yang and Levy v.1

$$F_s^{OL1} 1 + \frac{5}{27} s^2 + 0.00677 \frac{20}{3} (3\pi^2)^{-1/3} s \qquad (19)$$

- 30. GGA, Perdew

$$F_s^{P92} = \frac{1 + 88.396 s^2 + 16.3683 s^4}{1 + 88.2108 s^2} \qquad (20)$$

- 31. GGA, Vitos, Skriver, and Kollar (VSK)

$$F_s^{VSK98} = \frac{1 + 0.95x + 3.56x^3}{1 - 0.05x + 0.396x^2} \qquad (21)$$

with $x = (5/27)s^2$.

- 33. GGA, Ernzerhof

$$F_s^{E00} = \frac{135 + 28 s^2 + 5 s^4}{135 + 3 s^2} \qquad (22)$$

- 41. GGA, TB3

$$F_s^{TB3} = 1.20243339 s^{0.2} \qquad (23)$$

When I use the semilocal approximation, I have the following enhancement factor based on modifications of the second-order gradient expansion GE2

$$F_s^{GE2} = 1 + \frac{5}{-} s^2 + \frac{20}{27} q \qquad 9 \qquad (24)$$

or fourth-ordeer gradient expansion GE4

$$F_s^{GE4} = F_s^{GE2} + \Delta \qquad (25)$$

where Δ is

$$\Delta = \frac{8}{81} q^2 - \frac{1}{9} s^2 q + \frac{8}{243} s^4 \qquad (26)$$

GE4 functional, that is the simplest LL-meta-GGA functional, allows us to obtain better results for energy but the kinetic potential is divergent.

III. COMPUTATIONAL DETAILS

All the required numerical calculations have been performed using the electronic structure program: JELL-CODE. This program performs DFT simulations, both at the KS and the OF-DFT level, for spherical systems on a radial semi-logarithmic grid. A carefull calibration of the quadrature grid has been performed to ensure that all calculations are well converged. Varying the external potential, both atoms and jellium spheres can be considered.

IV. RESULTS

The main goal of mine is the development of new kinetic functionals which can be applied in different DFT applications. To reach this target, I have done several analysis with newly developed benchmark sets, which extend the previous ones; in the case:

- Jellium Cluster of 40 electrons,
- Jellium Cluster of 138 electrons,
- Noble Atoms (Ne, Ar, Kr, Xe, Rn, Og).

The Jellium Clusters of 40 and 138 electrons have type HOMO (highest occupied molecular orbital) p, later I have worked with Jellium Cluster of 92 electrons with type HOMO s and with Jellium Cluster of 254 electrons with type HOMO h. The noble atoms (He-Og) are used as representative of rapidly varying density systems. The jellium spheres (N=40e,138e) are used as representative of the slowly-varying density regime. The use of atoms and jellium spheres with varying numbers of electrons allows the consideration of both high- and low-density regime. After the energy studies exposed in the work[21], I also carried out studies on ionization, I plotted the ionization versus r_s, and I analyzed the trend of everyone functionals, as shown in Fig.1.
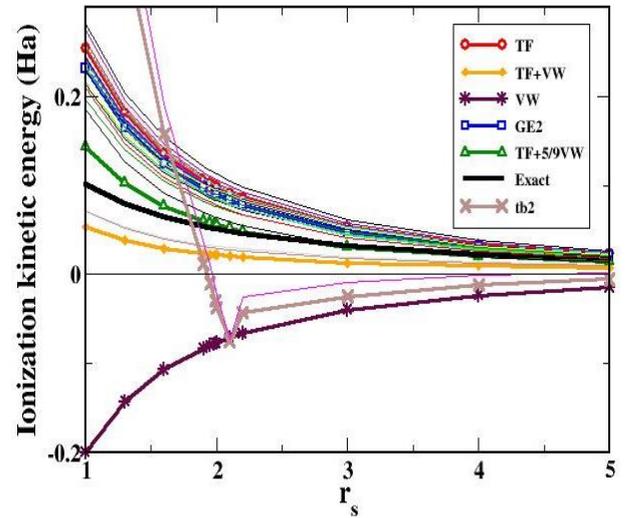
Fig. 1: The kinetic ionization calculated by the 41 kinetic functionals.

I have calculated the energy, the ionization and the potential for jellium clusters having different values of the bulk parameter, Wigner Seitz radius r_s,

$$r_s = \left(\frac{3}{4\pi\rho}\right)^{1/3} \qquad (27)$$

in particular in the range $r_s = [1,5]$ which corresponds to most metals and semiconductors[22]. The range [1,5] of values is expressed in atomic units that is, in units of the Bohr radius (as already done in Fig. 1).

From these graphs it can be seen that functional based on gradient expansions, e.g. the second-order one, GE2 have been found to work at best, see the Fig.1 and also in the Fig.2

Development of Novel Kinetic Energy Functional for Orbital-Free Density Functional Theory Applications-II
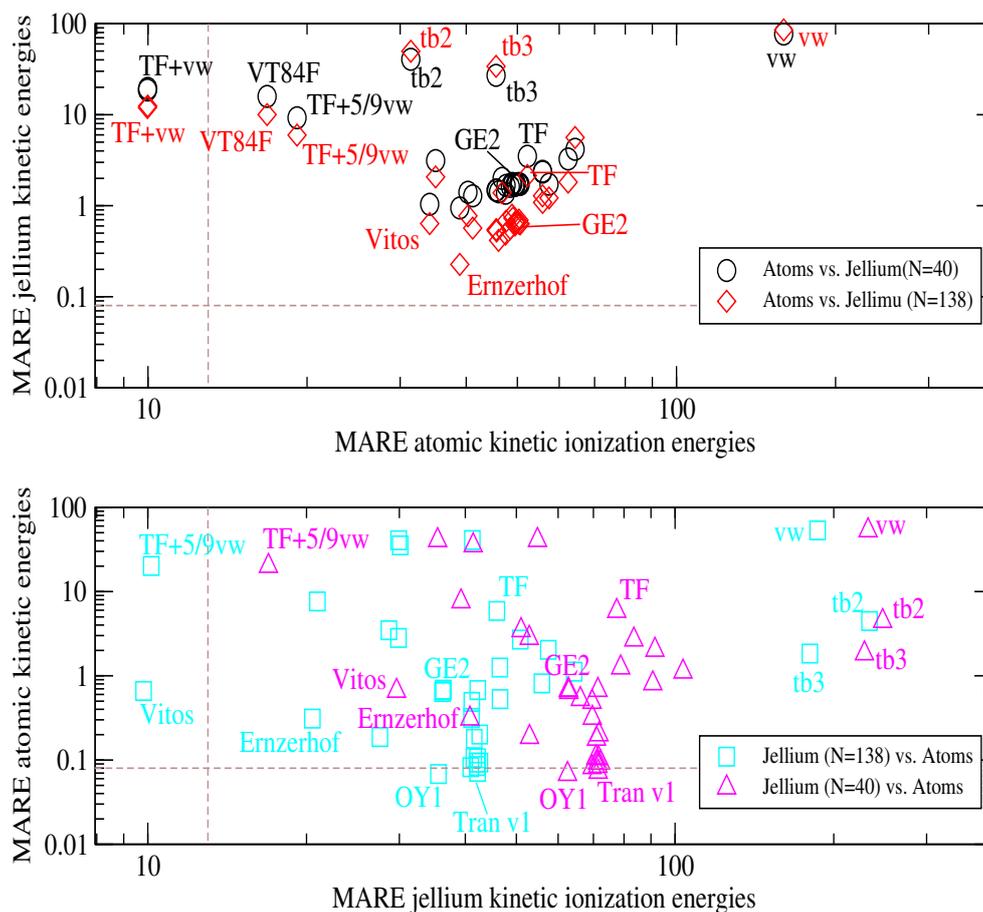
Fig. 2: Top: Mean Absolute Relative Error (MARE) of jellium kinetic energy (circle=sphere-40, rombus=sphere- 138) vs. MARE of noble atoms ionization kinetic en- ergy. Bottom: MARE of jellium ionization kinetic energy (square=sphere=138, triangle=sphere-40) vs. MARE of no- ble atoms kinetic energy.

This has motivated a further study, aimed at investigating the performance of the family of functionals

$$\lambda TF + \mu VW \tag{28}$$

with λ and μ being parameters.

The results of this study can be found in Figs. 4 and 5 of my work[21] for noble atoms and for the jellium spheres, respectively.

The following formulas are used for the relative errors

$$RelativeError_{energy} = \frac{Energy - Energy_{exact}}{Energy_{exact}} \tag{29}$$

$$RelativeError_{potential} = \frac{Potential - Potential_{exact}}{Potential_{exact}} \tag{30}$$

$$Kinetic\ Ionization\ Energy = T_{ion}[n] - T_{neutral}[n] \tag{31}$$

$$RelativeError_{ionization} = \frac{ionization - ionization_{exact}}{ionization_{exact}} \tag{32}$$

Plotting the enhancement factors both in GGA approximation and in LL-meta-GGA approximation (with GNU-PLOT), I obtained the results shown in the Fig. 6 of my work[21] and this confirms that the GGA approximation is not sufficient for our purposes but the LL-meta-GGA approximation works very well.

So, I have plotted the kinetic energy and the kinetic potential versus r of the functionals in approximation LL-meta-GGA and I found that the GE4 energy is the best, as shown in the Fig. 7[21], but the GE4 potential is divergent, as shown in Fig. 8[21] so I have developed new analytical formulas to eliminate this divergence.

Starting from the same functional form of the previous work:

$$F(s,q) = FW + FQ \tag{33}$$

I have obtained the following formula

$$F_s^{LAP1} = \frac{5}{3}s^2 + \frac{[1 + (A - 40/27)s^2]}{1 + As^2} * \frac{1 + 3q + Cq^2}{1 + Bq^2} \tag{34}$$

this functional has been built according to the exact constraints, i.e.

- for $s \to 0$ and $q \to 0$ (that is the slowly varying density limit) I want obtain the GE2 functional

- for $s \to \infty$ and $q \to \infty$ (that is the rapidly varying density limit) I want obtain the VW functional

The best values that I have obtained are

$$A = 1.70 \quad \text{and} \quad B = C \in [0, 0.10] \tag{35}$$

that allow us to get functionals that approximate the exact one very well both for energy and for potential

To obtain the coefficient A I have performed some scans with xfarbe program of the functional GE2 of which I know the energy and potential values, which are indicated below:

GE2	40e	92e	254e
energy	1.477	0.629	0.649
potential	10.974	9.602	6.7
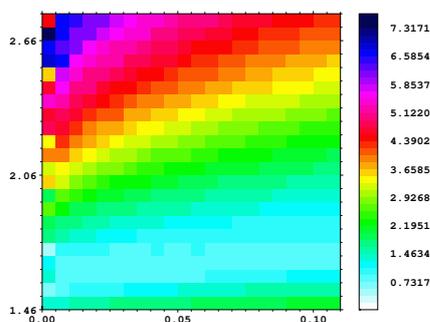
Fig. 3: Two dimensional scan for the GE2 functional over the parameter space A-B=C for the jellium of N=40e (mediated on rs=[1,5]) for the kinetic energy.
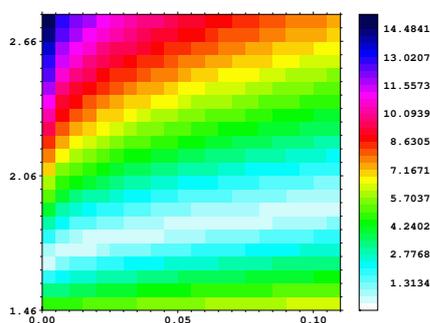
Fig. 4: Two dimensional scan for the GE2 functional over the parameter space A-B=C for the jellium of N=92e (mediated on rs=[1,5]) kinetic energy.
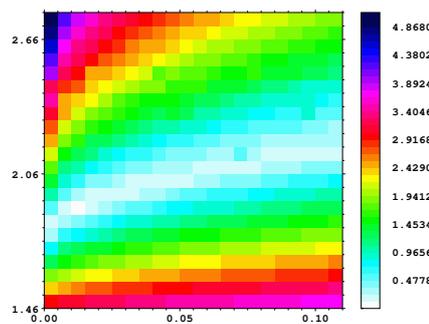
Fig. 5: Two dimensional scan for the GE2 functional over the parameter space A-B=C for the jellium of N=254e (mediated on rs=[1,5]) kinetic energy.

From these scans we can deduce that a good value for the coefficient A is $A = 1.70$, with which the following errors were calculated
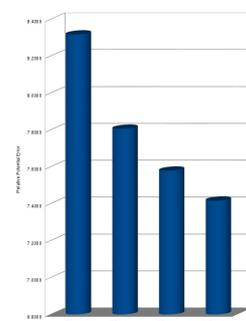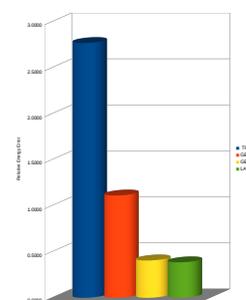
Fig. 6: Histogram of kinetic energy and kinetic potential errors, the new LAP1 functional with A=1.70 work very well.

Below are the 2D scans for the LAP1 functional in the B-C space with the coefficient $A = 1.70$. It can be seen that the right values for B and C are very small.

In the following plots it is possible to see the kinetic energy and the kinetic potential calculated with different functionals in particular the functional proposed in the other work[21] and the new LAP1 with a value of the co-

Development of Novel Kinetic Energy Functional for Orbital-Free Density Functional Theory Applications-II
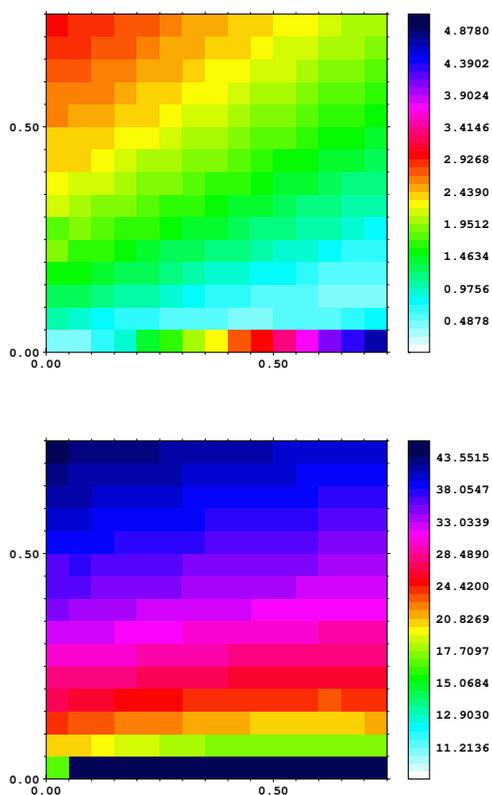
Fig. 7: Two dimensional scan for the LAP1 functional over the parameter space B-C for the 3 jellium's systems with A = 1.70: kinetic energy (in the upper panel) and kinetic potential (in the lower panel).

efficient $A = 2.06$ initially considered good but later improved.

In the following table there are the values of the errors on the energy and on the potential of the reference functionals and of the new functionals

Table I: Summary of MARE (Mean absolute relative errors)

Functional	KE error	KP error	total KE
TF	2.9618	24.8706	13.9162
GE2	0.954567	21.7619	11.3582
GE4	0.435183	10.6*10exp13	53.2*10exp13
NEWab	4.8922	24.3191	14,6056
LAP1	0.430675	16.3654	8.39804

In the following plots it is possible to see the kinetic energy and the kinetic potential calculated with different functionals in particular the functional proposed in the other work[21] and the new LAP1 with values of the coefficient $A = 1.70; 1.80$

In the following there are the 2D scans of the energy and potential above the space of the parameters $A - B = C$
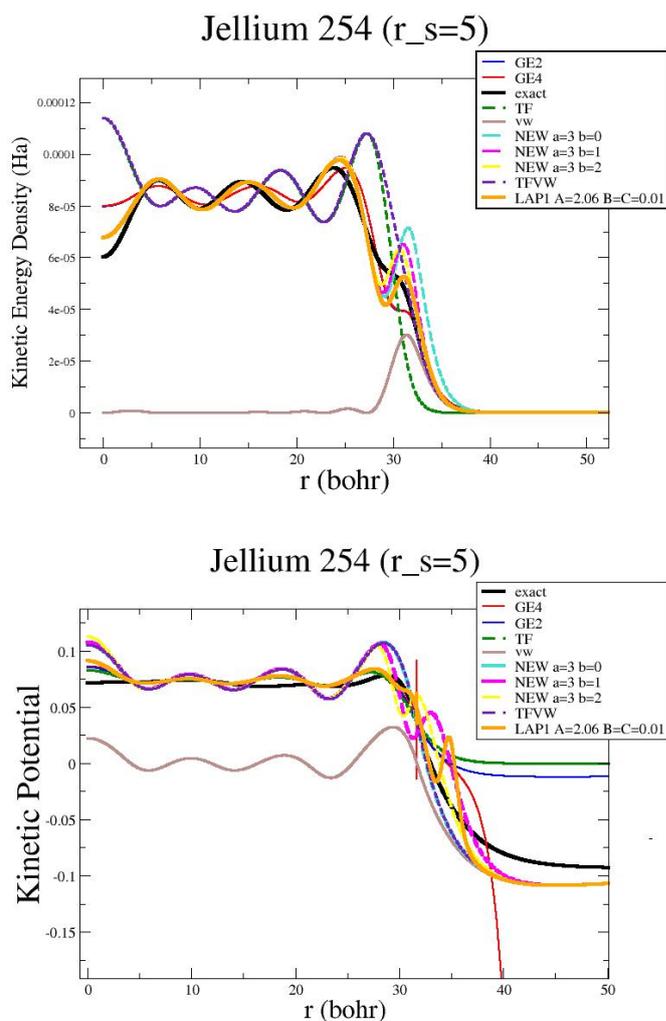
Fig. 8: In the upper panel there is the plot of the kinetic energy of some functionals and the new LAP1 one, in the lower panel there is the plot of the kinetic potential of same functionals and the new LAP1 one.
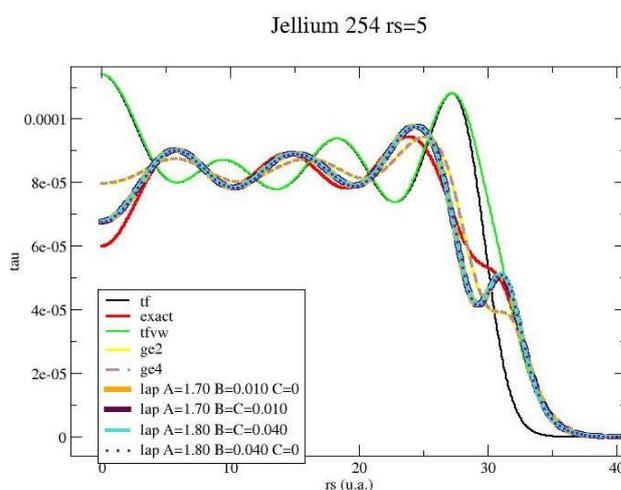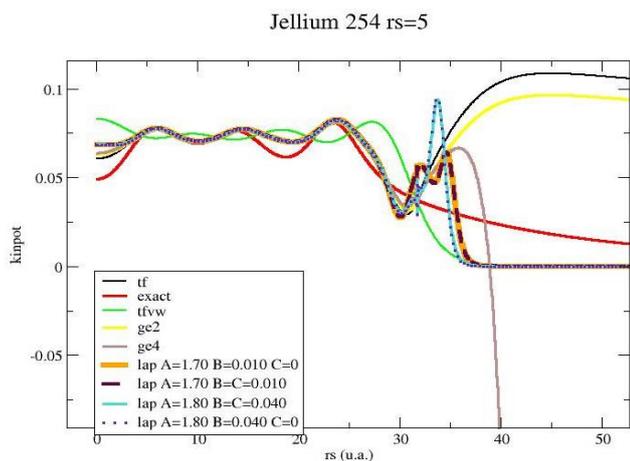
Fig. 9: The kinetic energies and the kinetic potential of some functionals and the LAP1 one.

for the function LAPI
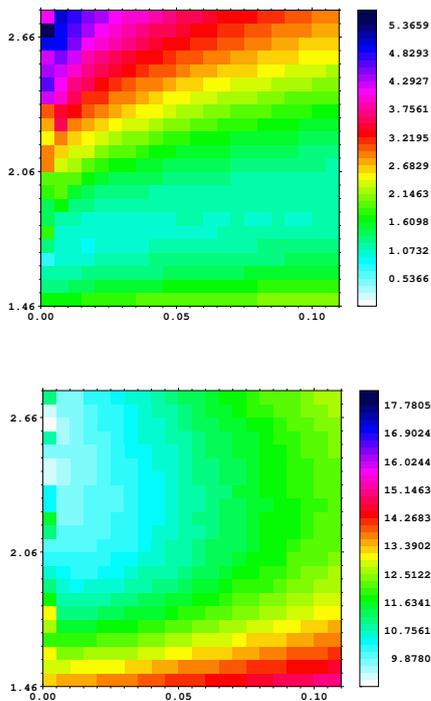
Fig. 10: Two dimensional scan for the LAP1 functional over the parameter A-B=C space for the jellium of 92e−, energy (in the upper panel) and potential (in lower panel).
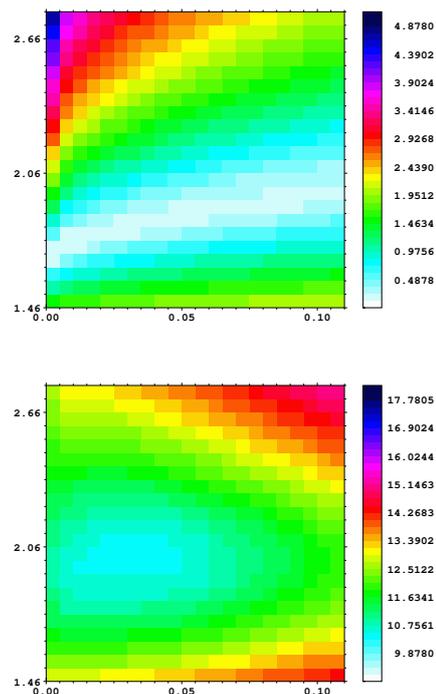
Fig. 11: Two dimensional scan for the LAP1 functional over the parameter A-B=C space for the jellium of 92e−, energy (in the upper panel) and potential (in lower panel).
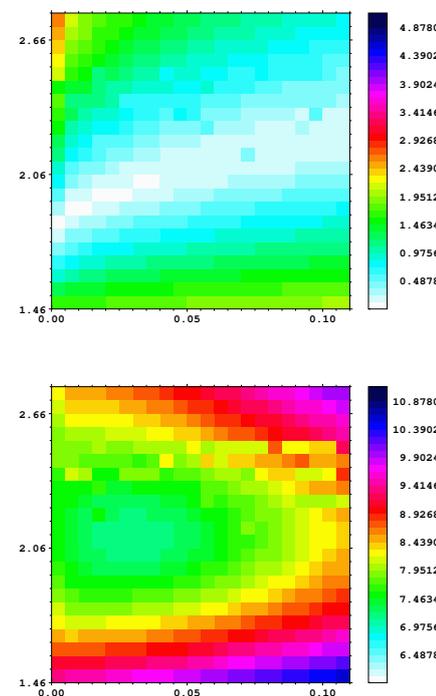
Fig. 12: Two dimensional scan for the LAP1 functional over the parameter A-B=C space for the jellium of 254e−, energy (in the upper panel) and potential (in lower panel).

London Journal of Research in Science: Natural and Formal

Development of Novel Kinetic Energy Functional for Orbital-Free Density Functional Theory Applications-II

V. CONCLUSIONS

The results that I obtained indicate the no GGA ki- netic energy functional available in literature is able to describe with good accuracy even simple systems such as noble gas atoms and jellium spheres. Nevertheless, gradi- ent expansions clearly include important features to ap- proximate the kinetic energy functional. Thus, I have in- vestigated the kinetic functionals beyond the GGA level of the theory, with special attention to LL-meta-GGAs, which can not only recover exactly gradient expansions but also describe rapidly-varying density regions, thanks to their ability to distinguish different density regions by virtue of the sue of both s and q. The results that I ob- tained, at a later time, indicate that no LL-meta-GGA ki- netic functional available in literature is able to describe with good accuracy the systems previously considered, in particular the potential of these systems. Nevertheless, with appropriate analyzes, functional devices can be ob- tained that are able to remove the divergences (where they exist), respecting the exact constraints and finding those parameters that can improve the errors of both energy and potential and eliminate oscillations, such as the functional LAP1 with the coefficient A = 1.70 and B = C ∈ [0, 0.10].

VI. DATA AVAILABILITY STATEMENT

All data generated or analysed during this study are included in this published article.

REFERENCES

1. E. Engel and R. M. Dreizler, Density functional theory (Springer, 2013).
2. Y. A. Wang and E. A. Carter, "Orbital-free kinetic- energy density functional theory," in Theoretical Methods in Condensed Phase Chemistry, edited by S. D. Schwartz (Springer Netherlands, Dordrecht, 2002) pp. 117–184.
3. T. A. Wesolowski and Y. A. Wang, Recent progress in orbital-free density functional theory, Vol. 6 (World Sci-entific, 2013).
4. H. Bruus and K. Flensberg, Many-body quantum theory in condensed matter physics: an introduction (Oxford univer-sity press, 2004).
5. L. H. Thomas, in Mathematical Proceedings of the Cam- bridge Philosophical Society, Vol. 23 (Cambridge Univer-sity Press, 1927) pp. 542–548.
6. W. Kohn and L. J. Sham, Phys. Rev. 140, A1133 (1965).
7. C. Ciraci and F. Della Sala, Physical Review B 93, 205405 (2016).
8. A. Krishtal, D. Sinha, A. Genova, and M. Pavanello, Jour- nal of Physics: Condensed Matter 27, 183202 (2015).
9. P. Elliott, K. Burke, M. H. Cohen, and A. Wasserman, Physical Review A 82, 024501 (2010).
10. J. Neugebauer, The Journal of Chemical Physics 126, 134116 (2007), https://doi.org/ 10.1063/ 1.2713754.
11. E. Fermi, Cl. Sci. Fiz. Mat. Nat 31, 21 (1922).
12. Y. A. Wang and E. A. Carter, in Theoretical methods in condensed phase chemistry (Springer, 2002) pp. 117–184.
13. V. V. Karasiev, R. S. Jones, S. B. Trickey, and F. E. Har- ris, New Developments in Quantum Chemistry , 25 (2009).
14. S. Laricchia, E. Fabiano, L. Constantin, and F. Della Sala, Journal of chemical theory and computation 7, 2439 (2011).
15. A. Lembarki and H. Chermette, Phys. Rev. A 50, 5328 (1994).
16. A. J. Thakkar, Phys. Rev. A 46, 6920 (1992).
17. J. P. Perdew and Y. Wang, Phys. Rev. B 45, 13244 (1992).
18. W. Yang, Phys. Rev. A 34, 4575 (1986).
19. S. Laricchia, L. A. Constantin, E. Fabiano, and F. Della Sala, Journal of chemical theory and computa- tion 10, 164 (2014).
20. S. Lehtola, C. Steigemann, M. J. Oliveira, and M. A. Marques, SoftwareX 7, 1 (2018).
21. V. Urso, "Development of novel kinetic energy functional for orbital-free density functional theory applications," (2021), https://doi.org/ 10.1142/S0129183122500449.
22. F. Tran and T. A. Wesolowski, "Semilocal approximations for the kinetic energy," in Recent Progress in Orbital-free Density Functional Theory, pp. 429–442.

A Grading Virtual Knots and its Applications

Myeong Ju Jeong

ABSTRACT

In 2013, Z. Cheng and H. Gao introduced the writhe polynomial of virtual knots by using coloring of Gauss diagrams and L. H. Kauffman introduced the affine index polynomial of virtual knots by using the Cheng coloring. In 2016, I introduced the zero polynomial of virtual knots, and in 2017, Z. Cheng generalized the writhe polynomial, the affine index polynomial and the zero polynomial. These invariants are obtained by deffining the weight of a crossing for a virtual knot diagram suitably. We give a grading of virtual knots by using the weights of crossings. This reveals a relationship between virtual knots and we can get grade tree diagrams of virtual knots. It enables us to compare virtual knots with many crossings more easily.

London Journals Press

A Grading Virtual Knots and its Applications

Myeong Ju Jeong

ABSTRACT

In 2013, Z. Cheng and H. Gao introduced the writhe polynomial of virtual knots by using coloring of Gauss diagrams and L. H. Kauffman introduced the affine index polynomial of virtual knots by using the Cheng coloring. In 2016, I introduced the zero polynomial of virtual knots, and in 2017, Z. Cheng generalized the writhe polynomial, the affine index polynomial and the zero polynomial. These invariants are obtained by deffining the weight of a crossing for a virtual knot diagram suitably. We give a grading of virtual knots by using the weights of crossings. This reveals a relationship between virtual knots and we can get grade tree diagrams of virtual knots. It enables us to compare virtual knots with many crossings more easily.

Keywords and phrases: virtual knot, writhe polynomial, affine index polynomial.

I. INTRODUCTION

We will grade virtual knots by using degrees of crossings in a virtual knot. It gives an invariant of virtual knots and grade tree diagrams of virtual knots which show relations between virtual knots. In this paper all knots and virtual knots are assumed to be oriented if it is not stated.

A. Henrich ([5]) defined a sequence of virtual knot invariants which are Vassiliev invariants of degree 1. In particular a polynomial invariant of virtual knots was obtained by taking the sum of terms after assigning a weight to each crossing.

Based on the Manturov's parity axioms ([10]), Z. Cheng ([1]) introduced an odd writhe polynomial $f_K(t)$ of virtual knots K, which is useful to distinguish some virtual knot from its inverse and mirror image. Z. Cheng considered the Gauss diagram of a virtual knot and used odd chords and coloring of arcs to define the polynomial. Z. Cheng and H. Gao ([3]) generalized the odd writhe polynomial to a polynomial $W_K(t)$.

L. H. Kauffman introduced the affine index polynomial of a virtual knot based on the Cheng coloring of a virtual knot diagram ([9]). An affine index polynomial $P_K(t)$ is given in the form

$$P_K(t) = \sum_c s(c)(t^{w_K(c)} - 1),$$

where $s(c)$ and $w_K(c)$ are the sign and the weight of a crossing c respectively. $W_K(t)$ and $P_K(t)$ differ slightly so that $W_K(t) = (P_K(t) + Q_K)t$, where Q_K is a numerical invariant of virtual knots arising from writhe ([3]).

The affine index polynomial cannot distinguish virtual knots if they are related by Δ-moves. If two virtual knots are related by a sequence of Δ-moves then they have the same value for Vassiliev invariants of degree less than 2 ([6]). Since the affine index polynomial gives us a sequence of Vassiliev invariants of degree 1, we may not distinguish two virtual knots which are related by Δ-moves. I introduced the zero polynomial to distinguish virtual knots which are not distinguished with the affine index polynomial([7]) and Cheng introduced a two variable function, associated to a virtual knot, which generalize the Henrich's polynomial, the odd writhe polynomial, the affine index polynomial and the zero polynomial ([2]).

L. H. Kauffman introduced virtual knots and showed many invariants of knots can be naturally extended for virtual knots. A virtual knot is a generalization of a knot and it is motivated from a knot in a thickened surface and from realizing Gauss code which needs virtual crossings ([8]). A *virtual knot diagram* is a knot diagram allowed to have virtual crossings, which are denoted by singular points surrounded by small circles as shown in Figure 1. The virtual knot diagram in Figure 1 has three crossings and one virtual crossing.
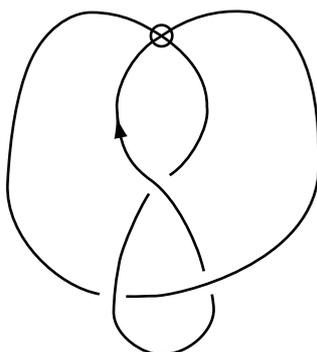
Figure 1.

We define the *sign* of a crossing of a virtual knot diagram as shown in Figure 2. A crossing is said to be *positive* (*negative*) if its sign is $+$ $(-)$. We denote the sign of a crossing c by $s(c)$. The *writhe* $w(K)$ of a virtual knot diagram K is defined to be the sum of signs of all crossings of K.

$$+1 \qquad\qquad -1$$

Figure 2: The sign of a crossing

The *Gauss diagram* of a virtual knot diagram K is defined to be an oriented circle with chords corresponding to crossings of K. The two endpoints of a chord correspond

to the preimages of the crossing of K. A chord corresponding to a crossing c is oriented from the preimage of the over crossing point of c to the preimage of the under crossing point of c. A chord is assumed to have the sign of the crossing corresponding to the chord. See Figure 3, which illustrates a virtual knot with two negative crossings c_1, c_2 and with a positive crossing c_3 and its Gauss diagram with three chords corresponding to the three crossings. We denote the Gauss diagram of K by $G(K)$. A virtual knot can be represented as a Gauss diagram and vice versa ([4, 8]).

K The Gauss diagram of K
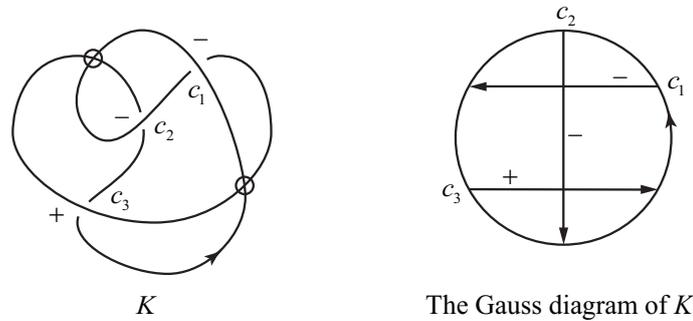
Figure 3

The moves of diagrams in Figure 4 and Figure 5 are called *Reidemeister moves* and *virtual moves* respectively.

A sequence of Reidemeister moves and virtual moves is called a *virtual isotopy*. A *virtual knot* is defined to be the virtual isotopy class of a virtual knot diagram. If there is a virtual isotopy between two virtual knot diagrams then they are said to be *equivalent* or *virtually isotopic*.
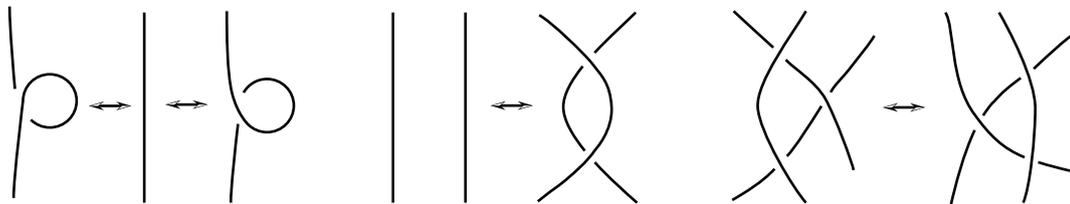
Figure 4: Reidemeister moves

A Gauss diagram G can be represented as virtual knot diagrams in many ways. All these virtual knot diagrams are virtually isotopic ([4]). In Gauss diagrams, the Reidemeister moves can be represented as a sequence of moves shown in Figure 6 ([4, 11]). From now on, ϵ in a Gauss diagram will denote the sign of a chord which can be either $+$ or $-$.

For each given virtual knot, we can get a grade tree diagram, which is invariant of virtual knots. In the grade tree diagram, usually we can get many simpler virtual knots obtained from the given one. If two virtual knots have many crossings then it can take much time to verify whether they are virtually isotopic or not. If we draw the grade tree diagrams of the two virtual knots, we can compare them more easily.
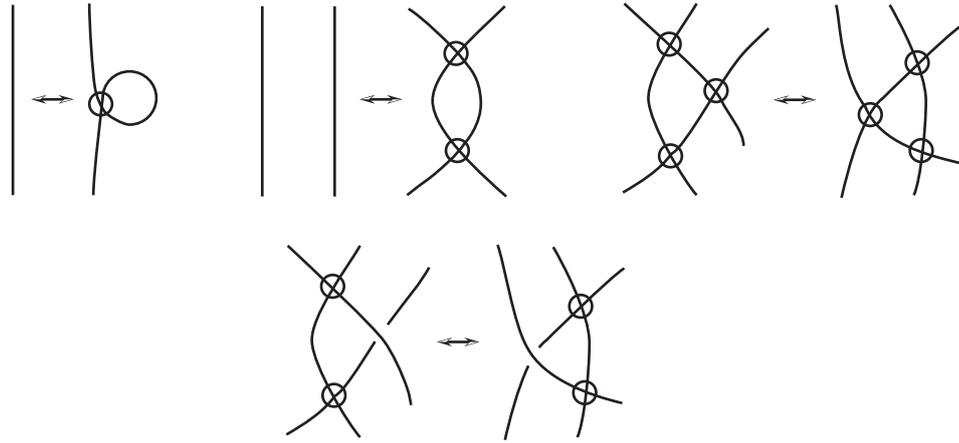
Figure 5: Virtual moves
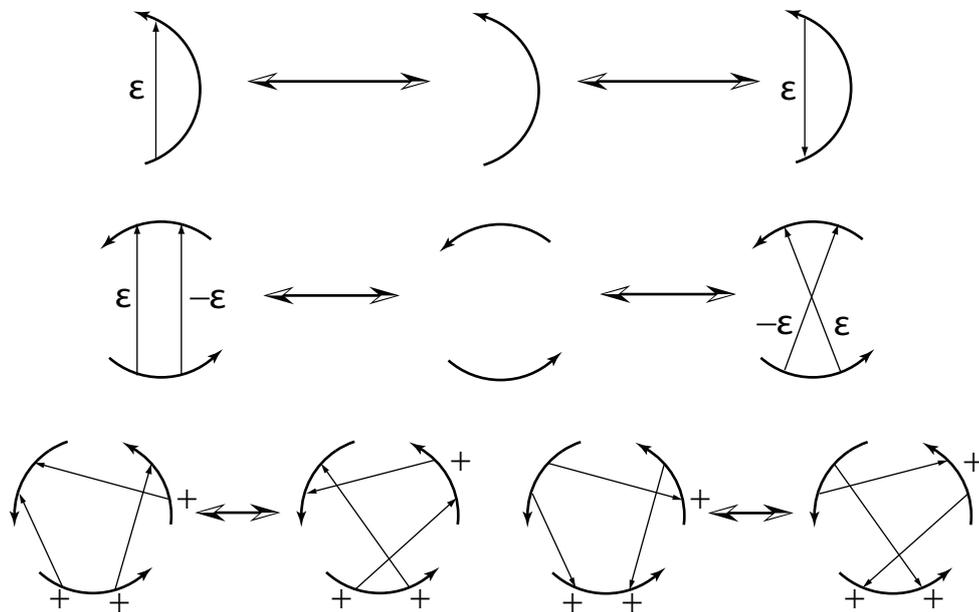
Figure 6: Moves in Gauss diagrams corresponding to Reidemeister moves.

In Section 2, we consider the degree of a crossing in a virtual knot K and grade virtual knots. For each natural number n, we get the virtual knot $V_n(K)$ obtained from K by virtualizing all crossings whose degrees cannot be divided by n. We show that $V_n(K_1)$ and $V_n(K_2)$ are equivalent if two virtual knots K_1 and K_2 are equivalent. We also show that for a virtual knot K and $n \in \mathbb{N}$, there exists a virtual knot K' such that K is equivalent to $V_n(K')$. By using connected sum of virtual knots, we show that for two given virtual knots K_1 and K_2, there is a virtual knot K' such that K_i is equivalent to $V_{n_i}(K')$ for $i = 1, 2$ if neither $n_1 | n_2$ nor $n_2 | n_1$. In Section 3, we give an example of using the grading to distinguish virtual knots and give a grade tree diagram of a virtual knot.

II. GRADING VIRTUAL KNOTS

Z. Cheng introduced an odd writhe polynomial by using Gauss diagrams and weights $\text{Ind}(c)$ of odd crossings c. We will slightly modify the weight $\text{Ind}(c)$.

Let c be a crossing of a virtual knot diagram K. For simplicity sake we will denote the chord of the Gauss diagram $G(K)$ corresponding to the crossing c by c too. For a chord c of a Gauss diagram, let r_+ and r_- be the numbers of positive chords and negative chords traversing c from left to right respectively and let l_+ and l_- be the numbers of positive chords and negative chords traversing c from right to left respectively. We define the *degree* $d(c)$ of a crossing c by the equation

$$d(c) = r_+ - r_- - l_+ + l_-.$$

Actually $d(c) = -\text{Ind}(c)$. For example, in Figure 7 we see that $d(c_1) = -3$ since $r_+ = 0$, $r_- = 2$, $l_+ = 1$ and $l_- = 0$. Similarly we can see that $d(c_2) = -2$, $d(c_3) = 0$ and $d(c_4) = -1$.
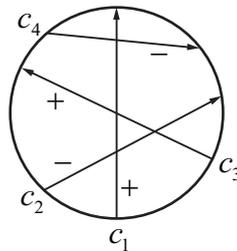
Figure 7

For a virtual knot diagram K, we denote the set of crossings of K by $C(K)$. For a natural number n, we define the set $C_n(K)$ of crossings of K as following

$$C_n(K) = \{c \in C(K) | d(c) \text{ is a multiple of } n\}.$$

By virtualizing all crossings of K whose degrees are not multiples of n, we get a virtual knot $V_n(K)$. For $n_1, \cdots, n_m \in \mathbb{N}$, $K(n_1, \cdots, n_m)$ is inductively defined as

$$\begin{cases} K(n_1) = V_{n_1}(K), \\ K(n_1, \cdots, n_m) = V_{n_m}(K(n_1, \cdots, n_{m-1})). \end{cases}$$

Let two virtual knot diagrams K_1 and K_2 be related by a Reidemeister move. Assume that d is a crossing of K_1 not involved with the Reidemeister move, then we denote the crossing of K_2 corresponding to d by d too. Similarly, in the Gauss diagrams $G(K_1)$ and $G(K_2)$, we use the same notation for the corresponding chords which are not involved with the Reidemeister move.

Now the polynomial $P_K(t)$ associated to K is defined by the equation

$$P_K(t) = \sum_{c \in C(K)} s(c)(t^{d(c)} - 1).$$

Theorem 2.1. [1, 9] $P_K(t)$ *is invariant under the Reidemeister moves.*

We will show that $V_n(K_1)$ and $V_n(K_2)$ are equivalent if two virtual knot diagrams K_1 and K_2 are related by Reidemeister moves.

Lemma 2.2. *Let two virtual knot diagrams K_1 and K_2 be related by a first Reidemeister move. Then $V_n(K_1)$ and $V_n(K_2)$ are equivalent for all $n \in \mathbb{N}$.*

Proof. Suppose that K_1 and K_2 differ by a first Reidemeister move and their Gauss diagrams are related as shown in Figure 8 or Figure 9. If $d \in C(K_1) - \{c\}$ then the degree of d coincides with that of the corresponding crossings of K_2. Since the degree of the chord c in the Figures is zero, c belongs to $C_n(K_1)$. Then we see that $V_n(K_1)$ and $V_n(K_2)$ are also related by a first Reidemeister move.
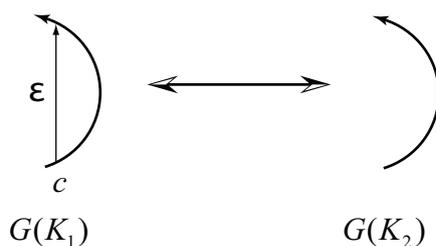
Figure 8
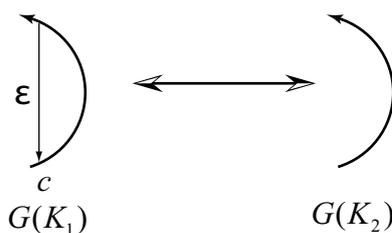
Figure 9

In [11], M. Polyak introduced four versions of the oriented second Reidemeister move as in Figure 10. The $\Omega 2a$ and $\Omega 2b$ moves can be represented as the move of Gauss
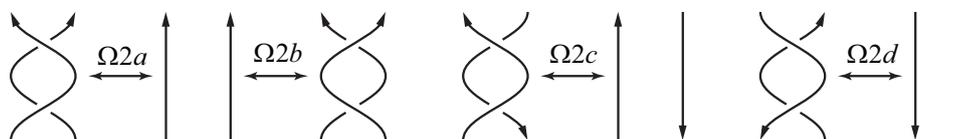
Figure 10

diagrams in Figure 11.

Lemma 2.3. *Let K_1 and K_2 be related by a second Reidemeister move. Then $V_n(K_1)$ and $V_n(K_2)$ are equivalent for all $n \in \mathbb{N}$.*

Proof. Suppose that K_1 and K_2 are related by the second Reidemeister move and their Gauss diagrams are as shown in Figure 11. If $d \in C(K_1) - \{c_1, c_2\}$ then the degree of d coincides with that of the corresponding crossing of K_2. Since $d(c_1) = d(c_2)$, we see that $c_1 \in C_n(K_1)$ if and only if $c_2 \in C_n(K_1)$. Hence $V_n(K_1)$ and $V_n(K_2)$ are equivalent. Similarly, we can show that it holds for the other versions of the oriented second Reidemeister move.
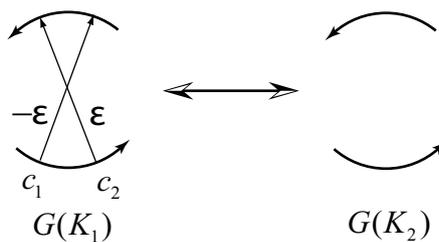
Figure 11

Lemma 2.4. *Let K_1 and K_2 be related by a third Reidemeister move. Then $V_n(K_1)$ and $V_n(K_2)$ are equivalent for all $n \in \mathbb{N}$.*

Proof. Suppose that K_1 and K_2 are related by the third Reidemeister move and their Gauss diagrams are related as shown in Figure 12. If

$$d \in C(K_1) - \{c_1, c_2, c_3\}$$

then the degree of d coincides with that of the corresponding crossings of K_2. So d belongs to $C_n(K_1)$ if and only if the corresponding crossing d' belongs to $C_n(K_2)$. By using the mathematical induction for the number of crossings, we can see that

$$d(c_1) = d(c_2) + d(c_3)$$

and

$$d(c_i) = d(c_i')$$

for $i = 1, 2, 3$. So the number $|\{c_1, c_2, c_3\} \bigcap C_n(K_1)|$ of elements in the set $\{c_1, c_2, c_3\} \bigcap C_n(K_1)$ is either 1 or 3.
If

$$|\{c_1, c_2, c_3\} \bigcap C_n(K_1)| = 1$$

then

$$|\{c_1', c_2', c_3'\} \bigcap C_n(K_2)| = 1$$

and $V_n(K_1)$ and $V_n(K_2)$ are equivalent.
If

$$|\{c_1, c_2, c_3\} \bigcap C_n(K_1)| = 3$$

7

then

$$|\{c_1', c_2', c_3'\} \bigcap C_n(K_2)| = 3$$

and $V_n(K_1)$ and $V_n(K_2)$ are related by the third Reidemeister move. So $V_n(K_1)$ and $V_n(K_2)$ are equivalent.

Similarly, we can show that it holds for the other versions of the oriented third Reidemeister move.
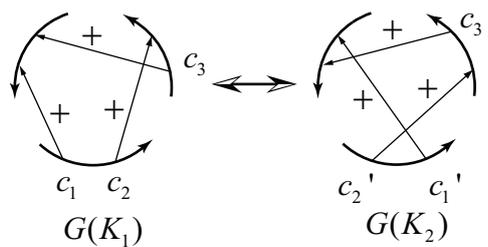
Figure 12

Combining Lemma 2.2, Lemma 2.3 and Lemma 2.4, we immediately get the following

Theorem 2.5. *If K_1 and K_2 are equivalent virtual knots then $V_n(K_1)$ and $V_n(K_2)$ are also equivalent for each $n \in \mathbb{N}$.*

By repeatedly applying Theorem 2.5 to virtual knots, we get the following

Corollary 2.6. *For natural numbers $n_1, \cdots, n_m$, if two virtual knots K_1 and K_2 are equivalent then $K_1(n_1, \cdots, n_m)$ and $K_2(n_1, \cdots, n_m)$ are also equivalent.*

Figure 13 illustrates that for a given virtual knot K how to construct a virtual knot K' such that K is equivalent to $V_3(K')$. We can add chords with degree ± 1 to change the degrees of the chords in K as desired. More generally we can get the following
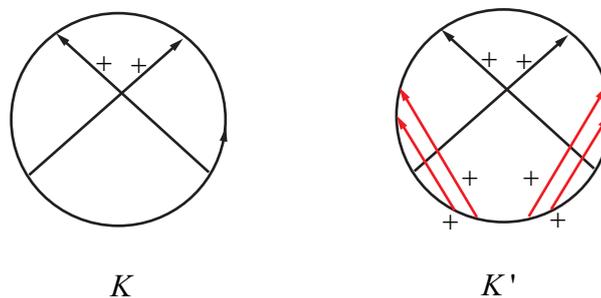
Figure 13.

Theorem 2.7. *For a virtual knot K and $n \in \mathbb{N}$, there exists a virtual knot K' such that K is equivalent to $V_n(K')$.*

Table I

crossing	c_1	c_2	c_3	c_4	c_5	c_6	c_7	c_8	c_9
degree	-4	0	5	6	1	4	0	-1	-3

If we consider the connected sum of virtual knots we can also show the following

Theorem 2.8. *Assume that the greatest common divisor of n_1 and n_2 is neither n_1 nor n_2. For two given virtual knots K_1 and K_2, there is a virtual knot K' such that K_i is equivalent to $V_{n_i}(K')$ for $i = 1, 2$.*

III. EXAMPLES

Let L be the virtual knot as shown in Figure 14. Then it has the trivial affine index polynomial. But $V_2(L)$ is a non-trivial virtual knot with $P_{V_2(L)}(t) = (t-1) + (t^{-1}-1) \neq P_O(t)$, where O is the trivial knot. So we see that L is non-trivial.

L $\qquad\qquad\qquad$ $V_2(L)$
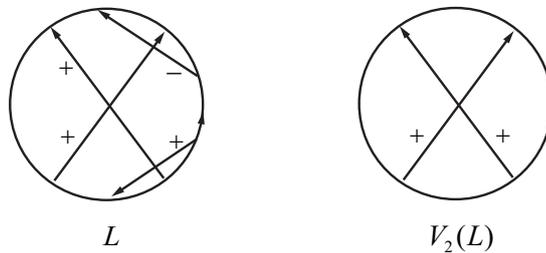
Figure 14

Let K be the virtual knot with nine crossings whose Gauss diagram is as shown in Figure 15.

K
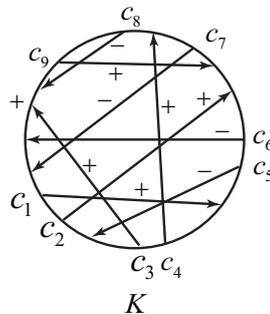
Figure 15

If we calculate the degree of crossings of K then we can get the Table 1.
Then we may get the grade tree diagram as shown in Figure 16.

London Journal of Research in Science: Natural and Formal
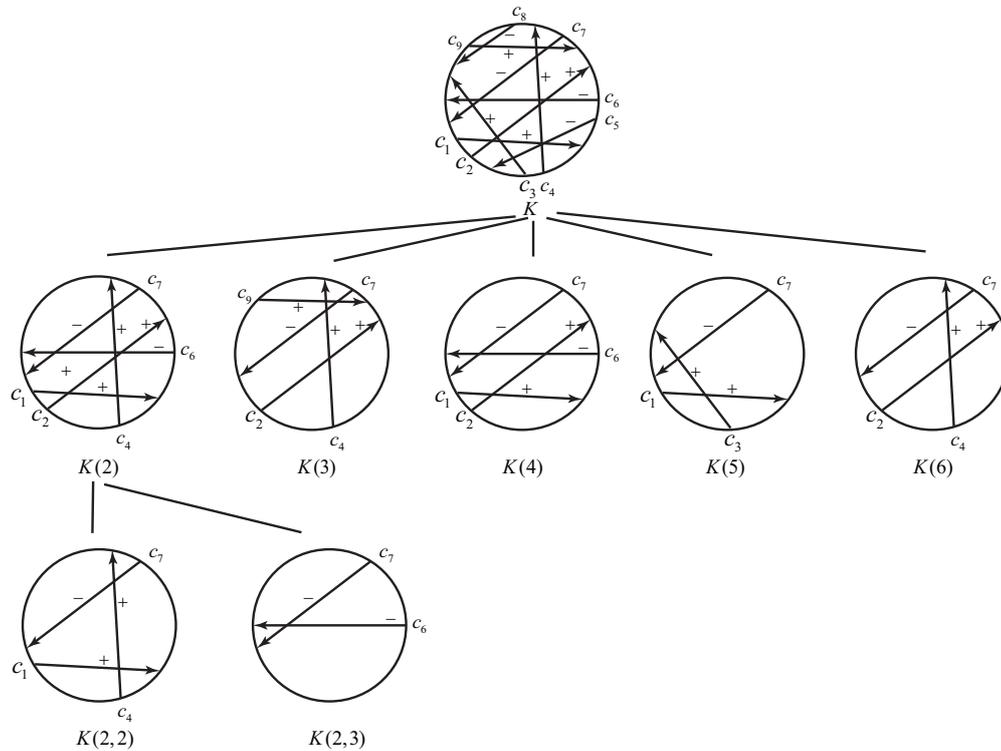
Figure 16

ACKNOWLEDGEMENT

REFERENCES

1. Z. Cheng, A polynomial invariant of virtual knots, Proc. Amer. Math. Soc. 142 (2014), No. 2, 713-725.
2. Z. Cheng, A transcendental function invariant of virtual knots, J. Math. Soc. Japan 69 (2017), No. 4, 1583-1599.
3. Z. Cheng and H. Gao, A polynomial invariant of virtual links, J. of Knot Theory and Its Rami_-cations 22 (2013), No. 12, 1341002, 33pp.
4. M. Goussarov, M. Polyak and O. Viro, Finite type invariants of classical and virtual knots, Topol-ogy 39 (2000), 1045-1068.
5. A.Henrich, A sequence of degree one Vassiliev invariants for virtual knots, J. of Knot Theory and Its Rami_cations 19 (2010), No. 4, 461-487.
6. M.-J. Jeong, Delta moves and Kau_man polynomials of virtual knots, J. of Knot Theory and Its Rami_cations Vol. 23 (2014), No. 10, 1450053, 17pp.
7. M.-J. Jeong, A zero polynomial of virtual knots, J. of Knot Theory and Its Rami_cations Vol. 25 (2016), No. 1, 15500784, 19pp.
8. L. H. Kauffman, Virtual knot theory, Europ. J. Combinatorics 20 (1999), 663-691.
9. L. H. Kauffman, An a_ne index polynomial invariant of virtual knots, J. of Knot Theory and Its Rami_cations Vol. 22 (2013), No. 4, 1340007, 30pp.
10. O. Manturov, Parity in knot theory, Sb. Math. 201 (2010), 693{733.
11. M. Polyak, Minimal generating sets of Reidemeister moves, Quantum Topology 1(4) (2010), 399-411.

London Journal of Research in Science: Natural and Formal

Effects of Climate Change on Real Estate Value

M. Farhaoui & Pr. C. Slimani

Sidi Mohamed Ben Abdellah University

ABSTRACT

The human activities are the main cause of climate change. The impact of this change is multiple on the environment such as: drought, water scarcity, salinization, frequent storms, glacier melting and sea level rising. Its impacts affects not only the whole population in the world but also the biodiversity. In addition, its negative effects are not limited to the environment; climate change touches the real estate in general and its value in particular.

Through this paper, the theme relating to the effects of climate change on the property value will be addressed. Indeed, the real estate market value is negatively affected by climate change impacts. Flooding, drought, water scarcity, water quality degradation, seal level rising are factors, which affect the property prices. An analytical approach is adopted to examine this issue based on laws texts, courts decisions, appraiser's reports and the research findings in the field.

The study is engaged in a legal doctrinal analysis of law and scientific research findings. It analyses decisions from courts and tribunals related to the impacts of climate change on property prices in order to establish their views of climate change consequences in determining real estate values and who bears the responsibility of property depreciation.

Keywords: climate change, effects, real estate appraisal, appraiser, property value.

Classification: DDC Code: 551.5112 LCC Code: TD885.5.G73

Language: English

Effects of Climate Change on Real Estate Value

Analyse D'impact des Changements Climatiques Sur la Valeur du Foncier

M. Farhaoui[α] & Pr. C. Slimani[σ]

ABSTRACT

The human activities are the main cause of climate change. The impact of this change is multiple on the environment such as: drought, water scarcity, salinization, frequent storms, glacier melting and sea level rising. Its impacts affects not only the whole population in the world but also the biodiversity. In addition, its negative effects are not limited to the environment; climate change touches the real estate in general and its value in particular.

Through this paper, the theme relating to the effects of climate change on the property value will be addressed. Indeed, the real estate market value is negatively affected by climate change impacts. Flooding, drought, water scarcity, water quality degradation, seal level rising are factors, which affect the property prices. An analytical approach is adopted to examine this issue based on laws texts, courts decisions, appraiser's reports and the research findings in the field.

The study is engaged in a legal doctrinal analysis of law and scientific research findings. It analyses decisions from courts and tribunals related to the impacts of climate change on property prices in order to establish their views of climate change consequences in determining real estate values and who bears the responsibility of property depreciation.

This topic is proposed to not only assess the influence of climate change on the real estate appraisal and provide land appraisers with necessary tools to take into account the impacts of climate change but also to prevent the policy makers on how this scourge affects the economy by decreasing the value of one of the most important sector.

RÉSUMÉ

Les changements climatiques ont pour origine principale les activités humaines sous la pression du commerce et de l'industrie. Ils se manifestent par une dégradation de l'environnement causant sécheresse, augmentation accrue de la salinité des sols, tempêtes fréquentes, fonte du glacier et élévation du niveau de mer. Ces impacts affectent l'ensemble de la population humaine ainsi que la biodiversité. Parmi les impacts néfastes sur l'environnement, nous voulons surtout attirer l'attention sur les effets négatifs sur le foncier en général et sur sa valeur en particulier.

A travers cet article, la question sur l'analyse d'impact des changements climatiques sur la valeur du foncier est soulevée avec tous ses enjeux et dimensions. En effet, la valeur du foncier peut diminuer à cause des inondations, de la sécheresse, de la salinisation des sols, de l'augmentation du niveau de mer et de la dégradation de la qualité de l'eau. Une approche analytique est adoptée pour traiter ce sujet en se basant sur le cadre juridique et jurisprudentiel, ainsi que les rapports d'expertise et les résultats de recherche dans ce domaine.

Ce thème est proposé pour non seulement évaluer l'influence des changements climatiques sur la valeur du foncier mais aussi pour mettre à la disposition des experts immobiliers les outils nécessaires et indispensables désormais pour tenir compte de l'impact de ces changements sur le marché immobilier devenu locomotive de toute économie en plein essor.

Mots-clés: changements climatiques, effets, expertise immobilière, expert, valeur du foncier.

It is worldwide accepted that the real estate business is one of the most important economic sectors in the world. Its value depends on many factors and appraisal approaches. Real estate appraisal is an issue of particular concern. It is the process of developing an opinion regarding the value of property based on the knowledge, experience, environment and professional assessment of value by real estate appraisers. The valuation is very subjective. To assess the property's value, it is crucial to assess the influence of factors on property market value.

Many factors can affect the property value such as physical factors: location, distance from center, features, conditions, facilities connections, environment (climate change in particular) and pollution. The second kind of factors is economic factors, which play a great role in real estate valuation such as supply and demand, interest rate, economic outlook, property market performance, investment potential. The third type of factors is social factors related to all social aspects, which affect the property market value such as demographic data, jobs …

Many studies have examined the effects of various factors on real estate values such as location, transportation, conditions, and homes features. However, the energy is not much analyzed as factor of real estate value despite its great role in determining the property values. The energy can be considered as a price setting factor in market price of real estate.

In this study, we focused on the impact of climate change on real estate appraisal in order to provide real estate appraiser tools to assess the property value taking into account the climate change

phenomenon and its impacts on property market value. Then, some sub-questions are asked like how climate change factors increase/decrease the property values? To which extend, climate change affects the real estate appraisal and appraisers reports? and does courts take into account the climate change disasters in determining the property value?

It is a difficult task to determine why real estate prices differ and how much this difference can be attributed to particular distinguishing features such as drought, sea level rising, temperature increasing and its relationships with other factors. The theme is very important in order to highlight climate change aspects that decrease the real estate market value and provide practitioners (judges, real estate appraisers, expert witness…) some rules to assess the property value according to the climate change factors.

This paper makes two contributions to the literature. First, the effects of climate change on real estate value are not well analyzed in the literature out of the US. Moreover, when it is explored it studies the effects on scientific point of view not in legally way. Second, previous studies examining the link between climate change and real estate price using scientific approaches. However, our research is the first to examine the effects of climate change on real estate using analytical approach by treasuring scientific research findings and regulatory framework associated with courts decisions in the field. To the best of our knowledge, there is a lack of systemic approach on the effects of climate change on property value.

This paper aims to provide important implications for policymakers, property investors, homeowners, buyers, sellers, real estate appraisers, courts all over the world about property losses due to climate change and its risks.

In real estate sector, there are many factors that increase or decrease the property market value. However, the risk is rising exponentially due to climate change and damage that can cause. Damages due to climate change are increasing and hit high records in the last decade in many

regions in the world. For example in the US, climate change such flood, mudslides and wildfires cost more than $300 billion in damage of residential and commercial properties[1]. Climate change appears a new wild card in real estate market that called the costs of climate change. Sea level rise and other impacts of climate change have received some previous interest in the literature. Then, many researches have noted a significant negative relationship between climate change and farmland values[2].

According to World Bank reports updated in October 2021, 132 million people will be pushed into poverty by climate change over the next 10 years; 216 million will be driven to migrate within their own countries by 2050. Natural disasters cost at least 390 billion a year due to wider disruption caused to households and firms. Moreover, according to the Washington post, june 24, 2014, $700 billion of coastal property could be below sea level by the end of the century and an additional $750 billion could be at high risk (high tides) without new policies against climate change.

Not all of this information are just alarming but they are the alarm bells for policymakers, real estate investors, homeowners, real estate appraisers because real estate business is most vulnerable for climate change.

The paper is organized in two sections. First section talks about directs effects of climate change on real estate value. However, the second section is analyzing the indirect effects of climate change on property market prices.

I. DIRECT EFFECTS OF CLIMATE CHANGE

1.1. *Rising sea levels*

Rising sea level could be the origin of two problems for homeowners, which affect negatively the property prices. The first is the high risk of temporary flooding events and the second is related to risk of seeing the site ultimately being flooded (underwater).

Since 1993, global sea level has increased by an average of 3.2 mm/year and it is projected to climb by another 0.26- 0.82 meters by 2100[3]. The ocean would increase by 39 inches and homes would be swamped by the end of the century in many coastal regions. Homeowners described this situation as a "death sentence for ever trying to sell house" according to the Washington post, June 24, 2014.

A study from the proceedings of the national Academy of sciences of the United States of America confirms that 200 million people worldwide will be displaced by 2100 because of rising sea levels.

The study conducted by Bernstein states that sea level rise decrease the homes prices by 7% than comparable homes. Moreover, this study warns about increasing of sales in high risk areas starting in 2013. Therefore, the same study shows that the value of properties exposed to sea level rise us depreciated by 7% than observably equivalent unexposed properties equidistant from the beach and 4% of discount among coastal properties not projected to be flooded for almost a century[4].

[1] Olick O., (2019), Climate values change will crush real estate for investors who don't prepare, new report says, https://www.cnbc.com/ 2019/04/08/climate-change-will-crush-real-estate-values-for-unprepared-investors-report.html, accessed 22/12/2021 at 14h41.

[2] Schlenker W., Hanemann M. W., Fisher A. C., (2005), Will US agriculture really benefit from global warming? Accounting for irrigation in the hedonic approach, American economic review, 95 (1), pp.395-406.

[3] Walsh P., Grffiths C., Guignet D., Klemick H., (2015), Adaptation, sea level, and property prices in the Chesapeake bay watershed, National center for environmental economics, U.S. environmental protection agency, pp.1-33.

[4] Bernstein A. Gustafson M. T., Lewis R., (2019), Disaster on the horizon: the price effect of sea level rise, Journal of financial economics, 134, pp.253-272.

Effects of Climate change on Real Estate Value

In addition, findings of some research indicate that the value of homes located in the threatened sea level rise areas, unprotected by adapted structures (bulkheads, ripraps, groin fields...) decreases by 19 to 23% on average. However, protected homes see its value increase by 21%[5]. Other research findings have confirmed that property values within 5 miles of the coast decrease about 10% in months plagued by red tide due to harmful algal blooms. Moreover, property prices drop 1-2% further for each additional month a bloom persists[6].

In addition, sunny day flooding is a new phenomenon related to climate change, which occurs without any precipitation and is driven only by lunar tides. This phenomenon causes losses to real estate values. For example, losses totaled $337 million from 2005 to 2017 in Miami[7].

The sea level rise is a factor that affects the real estate value. This factor is generally associated with flooding.

1.2. Flooding

Real estate market may be contorted by events such as flooding those changes the perceived importance of previously ignored risks[8]. The value of properties located in flood affected suburbs decreases because of flooding risks[9]. Moreover, Flood affects negatively the property value and influences immediately the rental property market[10].

Study conducted by Bin finds a significant price differentials after flooding events amounting from 6.0 to 20.5% for properties sold in flood zone[11].

The value of properties located in flood affected areas are really depreciated, this depreciation of value is about 9% regardless of the degree of damage caused by the storm[12]. Other research findings reveal a depreciation of flood plain property by 6.2% than an otherwise similar properties situated outside the flood plain if the property was sold before the flood plain maps were available if not, the depreciation rate becomes 2.3%[13]. In the same context, many researchers examine large concrete structure to be used in order to reduce erosion and reduce climate change risks.

Finally, Daniel et al find that an increase in flood risk of 1% in a year corresponds to 0.6% decrease of homes prices[14].

[5] Walsh P., Grffiths C., Guignet D., Klemick H., (2015), Adaptation, sea level, and property prices in the Chesapeake bay watershed, National center for environmental economics, U.S. environmental protection agency, pp.1-33.

[6] Berchard A., (2020), External costs of harmful algal blooms using hedonic valuation: the impact of Karenia brevis on southwest Florida, Environmental and sustainability indicators, 5, pp. 1-12.

[7] Rivera J., (2020) The Impact of Climate Change on Real Estate Valuations and Decisions, https://www.capright.com/the-impact-of-climate-change-on-real-estate-valuations-and-decisions-2/ accessed 22/12/2021 at 14h50.

[8] Lamond J., Proverbs D., Hammond F., (2010), The impact of flooding on the price of residential property : a transactional analysis of the UK market, housing studies, Vol. 25, N° 3, pp. 335-356.

[9] Rajapaksa D., Zhu M., Lee B., Hoang V., Wilson C., Managi S., (2017), The impact of flood dynamics on property values, Land use policy, 69, pp. 317-325.

[10] Eves C., Wilkinson S., (2014), Assessing the immediate and short-term impact of flooding on residential property participant behavior, Nat Hazards, 71, pp.1519-1536. Doi: 10.1007/s11069-013-0961-y

[11] Bin O., Landry C. E., (2013), Changes in implicit flood risk premiums : empirical evidence from the housing market, Journal of environmental economics and management, 65, 2013, pp.361-376.

[12] Ortega F., Taspinar S., (2018), Rising sea levels and sinking property values: hurricane sandy and New York's housing market, Journal of urban economics, pp.1-48. Doi: 10.1016/j.jue.2018.06.005.

[13] Samarasinghe O., Sharp B., (2010), Flood prone risk and amenity values: a spatial hedonic analysis, The Australian journal of agriculture and resource economics, 54, pp.457-475.

[14] Daniel V. E., Florax R., Rietveld P., (2009), Flooding risk and housing values: an economic assessment of environmental hazard, Ecological economics, 69, pp.355-365.

1.3. Drought

Climate conditions matter in housing, land prices and rents. Drought is an important factor that impacts negatively and significantly real estate value.

The research finds an evidence positive relationship between increase in reducing drought severity and property prices. A 1% increase in rainfalls is associated with up 0.07% increase in real estate price and 0.05% in rents. In addition, a 1% increase in temperature reduces the real estate value by up to 0.99% and rents by 0.55%[15].

Moreover, research conducted by Glaeser has confirmed that temperature and precipitation as climate-related amenity variables are very important demand-side determinants of real estate values[16].

Furthermore, the drought lets real investors use some adapted materials. Therefore, research finds that 1% increase in construction costs is associated with an increasing of housing prices, housing rents and land prices by 0.76%, 0.67% and 0.89% respectively[17].

The direct effects of climate change reduce the real estate value and increase the risks, which influence the property market price by affecting the offer and demand. Furthermore, the climate change has some indirect effects on real estate value.

II. INDIRECT EFFECTS OF CLIMATE CHANGE ON REAL ESTATE VALUE

2.1 Extreme weather

The climate change is the main cause of temperature increasing. Higher temperatures is not only the source of weather events but they increase the homes prices because higher temperatures is the cause of using more energy to air conditioning and fans and more water to keep lawns and landscaping alive[18].

Moreover, climate change factors such as extreme temperatures, temperature difference, precipitation, relative humidity have a significant and positive impact on housing in China[19].

In the same line, high global temperatures (longer summer heat waves) will extend the capacity of houses to air conditioning and increase utility costs. In addition, long periods of drought restrict building water usage and increase the chances of wildfires[20]. Therefore, that phenomenon requires a higher resiliency of building materials. As consequence, the costs of construction increase and the value of real estate will be seen increasing.

The temperature rising does not affect residential properties value in hot regions but also in cold areas where the snow is an amenity that increase the real estate value. Therefore, research findings have confirmed that the prices of residential properties located around ski resorts in the western United States and western Canada are

[15] Farzanegan R. M., Feizi M., Fereidouni G. H., (2019), Drought and property prices: empirical evidence from Iran, Marburg Centre for institutional economics, pp. 1-32.

[16] Glaeser E. L., Gyourko J., Saiz A., (2008), Housing supply and housing bubbles, Journal of urban economics, 64, pp.198-217.

[17] Farzanegan R. M., Feizi M., Fereidouni G. H., (2019), Drought and property prices: empirical evidence from Iran, Marburg Centre for institutional economics, pp. 1-32.

[18] Dehan A., (2021), How does climate change affect real estate prices?, https://www.rocketmortgage.com/learn/climate-change-real-estate-prices,accessed 22/12/2021 at 14h00.

[19] Huang D. J., Leung C. K., Qu B.,(2015), Do bank loans and local amenities explain Chinese urban house prices ?, China economic review, 34, pp. 19-38.

[20] Rivera J., (2020) The Impact of Climate Change on Real Estate Valuations and Decisions, https://www.capright.com/the-impact-of-climate-change-on-real-estate-valuations-and-decisions-2/accessed 22/12/ 2021 at 14h50.

Effects of Climate change on Real Estate Value

reduced due to global warming and reduction in snowfall intensity[21].

In addition of value depreciation caused by temperature increasing, this climate factor is almost responsible of wildfire, which affects the real estate value.

2.2 Wildfires

Wildfires have become a frightening reality in many countries of the world. Wildfires destroyed millions of hectares and thousands of structures last decade devastating people's houses. Therefore, this situation increases the real estate prices in the areas unaffected by fires[22].

Clayton, analyzing literature related to climate change, confirmed that the value of real estate decreases from 5% to 14% depending on the proximity to the fire[23]. This position is supported by supreme court state of north Dakota [24].

2.3 Algal blooms

Eutrophication phenomenon will be made worse by climate change. Climate change increases temperatures as is predicted to occur in many areas of the world. The blue green algae is more developed by both increased nutrients and high water temperatures and lakes with warm water. Moreover, the density of fish species eating zooplankton, microscopic animals very effective in controlling algae evolution, are higher in lakes and reservoirs with warm water[25].

Excessive level of nutrients and warm water stimulate harmful algal blooms, which are more severe and more difficult to be controlled due to warming caused by climate change.

Harmful algal blooms occur in reservoirs, lakes, dams and estuary at different levels. The first is related to high concentration of nutrients (Nitrogen and phosphorus in particular), warm water and adequate light. The second is associated with drought because of decreasing of the volume of lakes and reservoirs. Therefore, the concentrations of nutrients in water is higher and fish stir up more sediments. The third level is en relation with very hot and sunny days without cloud cover. Those days help harmful algal blooms to form just below or on the water surface. Algal blooms are as much as five times as severe in drought years as in wet years[26]. In general, drought influences the intensity of the harmful algal blooms in lakes, reservoirs, dams and estuary. Therefore, the harmful algal blooms affect the view and decrease the residential property prices as consequence.

A study performed in 2017 from Ohio state university estimated that algal blooms as result of warm weather cost Ohio homeowners who live near lakes $152 million from 2009 to 2015[27].

[21] Bustic V., Hanak E., Valletta R. G., (2011),Climate change and housing prices: hedonic estimates for ski resorts in western north America, Land economics, 87 (1), pp. 75-91.

[22] Dehan A., (2021), How does climate change affect real estate prices?, https://www.rocketm ortgage. com/learn/climate-change-real-estate-prices,accessed 22/12/2021 at 14h00.

[23] Clayton J., Devaney S., Sayce S. , Van De Weterin J., (2021), Climate risk and commercial property values: a review and analysis of the literature, UNEP FI available atunepfi.org/publications/investment-publications/cli mate-risk-and-commercial-property-values.

[24] Edwin Schulz vs Adam Helmers, Supreme case N°. 20210025, April 28, 2021.

[25] Havens K., (2018), The future of harmful algal blooms in Florida inland and coastal waters, TP-231, Sea grant college program, pp.1-4.

[26] Havens K., (2018), The future of harmful algal blooms in Florida inland and coastal waters, TP-231, Sea grant college program, pp.1-4.

[27] Williams G., (2019), How Climate Change Could Impact Your Home Value, https://realestate. usnews.com/real-estate/articles/how-climate-change-could-impact-your-home-value, accessed 22/12/2021 at 14h27.

III. CONCLUSION

Many studies have found that climate factors reduce property value. This study differs from above mentioned research in at least two reasons. First, the study uses an analytical approach of regulatory framework, research findings, real estate appraisers, courts decisions, and real estate reports. Second, it provides real estate practitioners with tools to be used in assessment of property value object of climate change impacts.

Climate change creates a high risks area: sea level rising, flooding, drought, temperatures increasing, harmful algal blooms. Those phenomena decrease the real estate value in one hand and increase the cost of construction in the other hand. Therefore, increased homeowner's insurance costs are observed in high risk areas.

Climate change does not only affect the property value but also induces many events increasing risks. Then homeowners pay more for insurance. The insurance premiums are raising when extreme weather events are likely repeated.

Also, drought, flooding, sea level rising, extreme weather are the main causes of degradation of the biodiversity. As consequence, groundwater is contaminated by sea water intrusion and soils salinization is observed. Moreover, surface water quality is degraded in addition of water quantity decreasing. All those factors induce de real estate value depreciation due to climate change.

REFERENCES

1. Berchard A., (2020), External costs of harmful algal blooms using hedonic valuation: the impact of Karenia brevis on southwest Florida, Environmental and sustainability indicators, 5, pp. 1-12.

2. Bernstein A. Gustafson M. T., Lewis R., 2019, Disaster on the horizon: the price effect of sea level rise, Journal of financial economics, 134, pp.253-272.

3. Bin O., Landry C. E., (2013), Changes in implicit flood risk premiums : empirical evidence from the housing market, Journal of environmental economics and management, 65, 2013, pp.361-376.

4. Bustic V., Hanak E., Valletta R. G., (2011),Climate change and housing prices: hedonic estimates for ski resorts in western north America, Land economics, 87 (1), pp. 75-91.

5. Clayton J., Devaney S., Sayce S. , Van De Weterin J., (2021), Climate risk and commercial property values: a review and analysis of the literature, UNEP FI available at –unepfi.org/publications/investment-publications/climate-risk-and-commercial-property-values.

6. Daniel V. E., Florax R., Rietveld P., (2009), Flooding risk and housing values: an economic assessment of environmental hazard, Ecological economics, 69, pp.355-365.

7. Dehan A., (2021), How does climate change affect real estate prices?, https://www.rocketmortgage.com/learn/climate-change-real-estate-prices, accessed 22/12/2021 at 14h00.

8. Eves C., Wilkinson S., (2014), Assessing the immediate and short-term impact of flooding on residential property participant behavior, Nat Hazards, 71, pp.1519-1536. Doi: 10.1007/s11069-013-0961-y

9. Farzanegan R. M., Feizi M., Fereidouni G. H., (2019), Drought and property prices: empirical evidence from Iran, Marburg Centre for institutional economics, pp. 1-32.

10. Glaeser E. L., Gyourko J., Saiz A., (2008), Housing supply and housing bubbles, Journal of urban economics, 64, pp.198-217.

11. Havens K., Effects of climate change on the eutrophication of lakes and estuaries, SGEF-189, Sea grant department, 2019, pp.1-3.

12. Havens K., (2018), The future of harmful algal blooms in Florida inland and coastal waters, TP-231, Sea grant college program, pp.1-4.

13. Huang D. J., Leung C. K., Qu B.,(2015), Do bank loans and local amenities explain Chinese urban house prices ?, China economic review, 34, pp. 19-38.

14. Lamond J., Proverbs D., Hammond F., (2010), The impact of flooding on the price of

residential property : a transactional analysis of the UK market, housing studies, Vol. 25, N° 3, pp. 335-356.

15. Olick O., Climate values change will crush real estate for investors who don't prepare, new report says, https://www.cnbc. com/2019/04/ 08/climate-change-will-crush-real-estate-value s-for-unprepared-investors-report.html, accessed 22/12/2021 at 14h41.

16. Ortega F., Taspinar S., (2018), Rising sea levels and sinking property values: hurricane sandy and New York's housing market, Journal of urban economics, pp.1-48. Doi: 10.1016/ j.jue.2018.06.005

17. Rajapaksa D., Zhu M., Lee B., Hoang V., Wilson C., Managi S., (2017), The impact of flood dynamics on property values, Land use policy, 69, pp. 317-325.

18. Rivera J., (2020) The Impact of Climate Change on Real Estate Valuations and Decisions,https://www.capright.com/the-impa ct-of-climate-change-on-real-estate-valuations- and-decisions-2/ accessed 22/12/2021 at 14h50.

19. Samarasinghe O., Sharp B., (2010), Flood prone risk and amenity values: a spatial hedonic analysis, The Australian journal of agriculture and resource economics, 54, pp.457-475.

20. Schlenker W., Hanemann M. W., Fisher A. C., (2005), Will US agriculture really benefit from global warming? Accounting for irrigation in the hedonic approach, American economic review, 95 (1), pp.395-406.

21. The Washington post, on NC's outer banks, scary climate-change predictions prompt a change of forecast, jun 24, 2014 accessed 09/01/2022 at 19h09

22. Walsh P., Grffiths C., Guignet D., Klemick H., 2015, Adaptation, sea level , and property prices in the Chesapeake bay watershed, National center for environmental economics, U.S. environmental protection agency, pp.1-33.

23. Williams G., (2019), How Climate Change Could Impact Your Home Value, https://realestate.usnews.com/real-estate/arti cles/how-climate-change-could-impact-your-h ome-value, accessed 22/12/2021 at 14h27.

Assessing the Antifungal Activities of *Buchholzia coriacea* on Dermatophytes Isolated from Horses in Katsina State, Nigeria

C.A. Salami, I.J. Omeh, S. Lukman & C.N. Kwanashie

University of Maiduguri

ABSTRACT

Dermatophytes are filamentous fungi that affect both human and animal skin, hair, and nails. There is a public health issue with it. In order to ascertain the effects of the methanolic extracts of Buccholzia coriacea on the isolates and the sensitivity level of the isolates to common antifungal drugs, this study was developed to explore the prevalence of Dermatophytes from clinical cases in horses. Samples were initially cultivated on Sabouraud dextrose agar, and then on Potato dextrose agar (secondary culture). Twelve (12%) of the sixty (60) clinical samples that were obtained were positive for Dermatophytes. T. rubrum (1), T. verrucosum (3), T. equinum (3), M. audounii (2), and M. gypseum (3) were the species recognized. At concentrations between 125 and 250 mg/ml, the methanolic extract of Buccholzia coriacea demonstrated antifungal effects on every isolate with values for the minimum inhibitory concentration (MIC) and minimum fungicidal concentration (MFC). The isolates' susceptibility to six popular antifungal medications was assessed. The isolates were well inhibited by Ketoconazole and terbinafine, but none of them were susceptible to amphotericin B. This study was able to show that Buccholzia coriacea's methanolic extract has antifungal properties. Additionally, two Dermatophytes species (Trichophyton and Microsporum) from Katsina state, Nigeria, were able to be isolated for this study.

London Journals Press

Assessing the Antifungal Activities of *Buchholzia coriacea* on Dermatophytes Isolated from Horses in Katsina State, Nigeria

C.A. Salami[α], I.J. Omeh[σ], S. Lukman[ρ] & C.N. Kwanashie[ᴄᴏ]

ABSTRACT

Dermatophytes are filamentous fungi that affect both human and animal skin, hair, and nails. There is a public health issue with it. In order to ascertain the effects of the methanolic extracts of Buccholzia coriacea on the isolates and the sensitivity level of the isolates to common antifungal drugs, this study was developed to explore the prevalence of Dermatophytes from clinical cases in horses. Samples were initially cultivated on Sabouraud dextrose agar, and then on Potato dextrose agar (secondary culture). Twelve (12%) of the sixty (60) clinical samples that were obtained were positive for Dermatophytes. T. rubrum (1), T. verrucosum (3), T. equinum (3), M. audounii (2), and M. gypseum (3) were the species recognized. At concentrations between 125 and 250 mg/ml, the methanolic extract of Buccholzia coriacea demonstrated antifungal effects on every isolate with values for the minimum inhibitory concentration (MIC) and minimum fungicidal concentration (MFC). The isolates' susceptibility to six popular antifungal medications was assessed. The isolates were well inhibited by Ketoconazole and terbinafine, but none of them were susceptible to amphotericin B. This study was able to show that Buccholzia coriacea's methanolic extract has antifungal properties. Additionally, two Dermatophytes species (Trichophyton and Microsporum) from Katsina state, Nigeria, were able to be isolated for this study.

Keywords: dermatophytes, *buccholzia coriacea,* methanolic extract, antifungal drugs, horses.

Author α: Department of Agricultural Technology, School of Applied Sciences Federal Polytechnic Nasarawa, Nigeria.

σ: Department of Veterinary Physiology and Biochemistry, Faculty of Veterinary Medicine. University of Maiduguri, Borno State Nigeria.

ρ: Department of Veterinary Public Health and Preventive Medicine, Faculty of Veterinary Medicine University of Abuja, Nigeria.

ᴄᴏ: Department of Veterinary Microbiology, Faculty of Veterinary Medicine. Ahmadu Bello University Zaria, Nigeria.

I. INTRODUCTION

Skin disease known as dermatophytosis is brought on by a group of fungus that are morphologically and physiologically related (Mihali *et al.,* 2012). It is well recognized that dermatophytes can infect keratinized tissues like skin, hair, and nails with fungus. The three genera that these organisms fall under are Trichophyton, Epidermophyton, and Microsporum.

According to host preference and natural habitat, dermatophytes are further divided into three groups: zoophilic species, which typically infect non-human mammals, geophilic species, which are soil-based and may also infect both humans and animals, and anthropophilic species, which primarily infect humans (Gupta *et al.,* 2003).

The virulence of the infecting strain or species, the host's response to the metabolic byproducts of the fungus, the anatomic location of the infection, and local environmental conditions are some examples of the elements that affect the severity of the infection. Alopecia with erythema, ranging from mild to severe, is typically one of the clinical symptoms (Chermette *et al.,* 2008). The majority

of the time, lesions are not pruriginous. However, kerion and miliary dermatitis, which rapidly spread from the saddle and girth through the body, can also happen (Chermette *et al.,* 2008).

In nail infections (onychomycosis), the nail may become thick, develop white patches, or even become dystrophic and split from its bed (Degreef, 2008). Dermatophyte infections are often limited to the superficial epidermis, but in immunocompromised patients, these fungi can be invasive and result in a severe and widespread infection, leading to the development of dermatophytic granulomas (Rodwell *et al.,* 2008).

Stallions in particular play a significant role in Nigeria's sociocultural activities with regard to horses. They are also preserved by mounted police and the army for security operations, as well as being utilized for recreational riding, polo, racing, durbar, and traditional festivities (RIM, 1992). Dermatophytoses are an example of a superficial fungal skin infection that can be zoonotic and pose a major health risk (Nweze *et al.,* 2007). Data on the number and types of Dermatophytes in Daura, Katsina State, are to be provided by this study.

It further attempts to assess the effectiveness of plant extracts in the treatment of dermatophytosis in light of rising medication resistance concerns.

II.   MATERIALS AND METHODS

2.1 Study Area

Daura is a local government in Katsina state, Northern Nigeria. Its GPS location is Latitude 11° 33'14.76"N and Longitude 11° 24'21.60" E with an estimated population of 78,277.

2.2 Sampling and Sample Size

Purposive sampling was employed, with availability and sampling time taken into consideration. From several farms, residences, and horse stables in the Daura Local Government area, sixty (60) skin scrapings and hair samples were collected from both clinical instances of Dermatophytoses in horses between March and June.

2.3 Sample Collection

Using 70% alcohol to clean and disinfect the lesions, skin scrapings and swabs, as well as plucked hair, were gathered from the edges of the lesions (Elewski, 2000). Hairs were pulled out and removed (Quinn *et al.,* 1994). All acquired animal samples came with information about the animals' age, sex; anatomical sites where samples were taken, as well as the date the samples were taken. There was no previous antifungal therapy.

2.4 Direct Microscopic Examination of Samples

On a microscope slide, little amounts of each scraping were put, and 1–2 drops of 10% potassium hydroxide were added. According to Hainer's description (2003), a cover slip was put on and the slide was slowly heated over a flame. Each treated slide was meticulously inspected for the presence of diagnostic fungi characteristics using low (x10) and high (x40) power objectives.

2.5 Laboratory Culture of Dermatophytes

For primary isolation, Sabouraud dextrose agar (SDA) (Oxoid, UK), a selective media containing cycloheximide (500 mg/L), nicotinic acid (100 g/ml), and chloramphenicol (40 mg/L), was utilized. Most molds and yeasts are inhibited by cycloheximide, bacteria are killed by chloramphenicol, and Trichophyton equinum grows when nicotinic acid is present (Raymond and Piphet, 2008). The material was added to the SDA plates, which were then incubated for one to four weeks at room temperature.

2.6 Identification of Isolates

On Potato Dextrose Agar (PDA) (Oxoid, UK), suspected growths were sub-cultured in order to promote the synthesis of unique spores for identification and pigment production. For one to four weeks, the subcultures were incubated at room temperature (Raymond and Piphet, 2008). After staining with lactophenol cotton blue and utilizing the Fungal colour atlas, the colony (obverse and reverse morphology) and microscopic features were used to identify the species (Barros, 2007).

Assessing the Antifungal Activities of Buchholzia Coriacea on Dermatophytes Isolated from Horses in Katsina State, Nigeria

28   Volume 22 | Issue 12 | Compilation 1.0   © 2022 London Journals Press

2.7 Preparation of Inoculums

To improve the formation of pure cultures, freshly grown cultures on the SDA were sub-cultured on Potato Dextrose Agar (PDA) plates for 4 days. A sterile loop was then used to harvest the growth. The suspension was then homogenized by shaking, allowed to settle for twenty minutes, and then its opacity was corrected with sterile distilled water to match a reference control (0.5McFarland standard).

2.8 Antifungal Activity of the Extracts

The extracts were diluted with distilled water to create a stock solution containing 1000 mg/ml of the extracts. For each set of labeled, sterile test tubes containing the different isolates, 4.5 ml of SDA broth was added. Using a sterile syringe and 0.5ml of the extracts drawn from the stock solution, a two-fold serial dilution was performed. A positive and negative control was set up, and both of them were cultured at room temperature for 24-48 hours before being monitored. Growth or cloudiness indicators were noted as negatives, while a lack of growth or cloudiness was noted as favorable. For the purpose of determining the minimum inhibitory concentration (MIC) and minimum fungicidal concentration, those lacking cloudiness or growth were cultivated on sterile SDA plates (MFC).

2.9 Antifungal Susceptibility Test Procedure

Seven antifungal medications were tested: Griseofulvin, 10 mg (Liofilchem, Italy), Ketoconazole, 50 mg (Liofilchem, Italy), Itraconazole, 50 mg (Liofilchem, Italy), Terbinafine, 100 mg (Novartis Research Institute, Vienna, Austria), and Amphotericin B, 20 mg (Liofilchem, Italy) (Liofilchem, Italy). Based on the technique reported by Esteban *et al.,* (2005)

on Agar-based disk diffusion susceptibility for Dermatophytes. It was applied to Petri dishes containing Mueller Hinton agar medium using the inoculums created for testing the extracts, distributed using a sterile swab, and allowed to air dry for five minutes in a safety cabinet. After being put to the plates with sterile forceps, the antifungal discs were incubated at room temperature for up to 5 days, at which point the zones of inhibition were visible. These were measured using a ruler for each antifungal agent and recorded (Penduka *et al.,* 2011).

2.10 Statistical Analysis

To provide a clear and accurate understanding of the outcomes, some statistical analysis was done on the data gathered from the field survey and laboratory study. The Chi-square test and the Descriptive Statistics of Cross-tabulation (Cross-tab) are examples of statistical techniques. The cross distributions of two separate outcomes were displayed using the cross-tab. The degree of independence between two groups was tested using the Chi-square. Additionally, some of the statistics were shown as graphs and tables. The statistical analysis was performed using the Statistical Package for Social Science (SPSS) version 20.0 software.

III.   RESULTS

60 clinical samples altogether were cultivated for dermatophytes, 12 (20%) were isolated and recognized as such. Trichophyton (7) and Microsporum (5) were isolated and characterized (Table 1). The additional fungi that were isolated from the samples were Rhizopus, Mucor, Yeast, and Aspergillosis.

Table 1: Number of Dermatophytes Isolates and Other Fungi from Horses

Species	Frequency	Percent
Dermatophytes	12	20.0
Other fungi	48	80.0
Total	60	100.0

Assessing the Antifungal Activities of Buchholzia Coriacea on Dermatophytes Isolated from Horses in Katsina State, Nigeria

© 2022 London Journals Press

Volume 22 | Issue 12 | Compilation 1.0   29

London Journal of Research in Science: Natural and Formal

Table 2: Dermatophytes Isolated from Horses

		Isolates			Total
		Other Fungi	*Microsporum*	*Trichophyton*	
Horses	Count	48	5	7	60
	% within	80.0	8.3	11.7	100.0

Cross Tabulation

The distribution of the isolates among the major sample-related parameters was ascertained using the cross-tab calculated. These variables include the samples' age, anatomical locations, and gender. This would allow the investigation to identify the areas with the highest concentrations of isolates among the aforementioned criteria.

Table 3: Age Distribution in Relation to Isolation Rate of Dermatophytes

Age			Isolates	
			Microsporum	*Trichophyton*
	1-5 yrs	Count	1	2
		% within isolates	20.0	28.6
	6-10 yrs	Count	3	4
		% within isolates	60.0	57.1
	11-15 yrs	Count	1	0
		% within isolates	20.0	0
	16-20 yrs	Count	0	1
		% within isolates	0	14.3
			5	7

Table 4: Anatomical Site and Dermatophytes Isolates

Anatomical site		Isolates	
		Microsporum	*Trichophyton*
Head	Counts	1	1
	% within isolates	20	14.3
Neck	Count	2	1
	% within isolates	40	14.3
Back	Count	2	4
	% within isolates	40	57.1
Limbs	Count	0	1
	% within isolates	0.0	14.3
Total		5	7
		100.0%	100.0%

Table 5: Sex and Dermatophytes Isolates Distribution

Sex		Isolates	
		Microsporum	*Trichophyton*
Male	Count	3	5
	% within isolates	60.0	71.4
Female	Count	2	2
	% within isolates	40.0	28.6
Total		5	7
		100.0	100.0

Assessing the Antifungal Activities of Buchholzia Coriacea on Dermatophytes Isolated from Horses in Katsina State, Nigeria

30   Volume 22 | Issue 12 | Compilation 1.0   © 2022 London Journals Press

The distribution of anatomical sites, ages, and statistical differences between the isolates were examined using the chi-square test. Additionally, it is used to determine whether each of the components inside a factor, such as anatomical site, is independent of the other. For instance, it is used to determine whether the occurrence of isolates (Microsporum and Trichophyton) on the head is independent of the occurrence on the neck.

Table 6: Chi-Square Test Statistics

Relationships	Chi-square value	P value
Isolates and Anatomical sites	12.059	0.061
Isolates and Age	6.301	0.39
Isolates and Categories	1.542	0.463
Isolates and Sex	138	0.933

Table 7: Results of Antifungal Activity of *Buchholzia coriacea* on the Dermatophytes Isolate

Dermatophytes	Isolates	MIC(mg/ml)	MFC(mg/ml)
Microsporum audounii			
A	HM10	125	250
B	HM13	125	250
Microsporum gypseum			
A	HM3	125	250
B	HM8	125	250
C	HF50	125	250
Trichophyton rubrum			
A	HM58	125	125
Trichophyton verrucossum			
A	HM39	125	125
B	HM45	125	250
C	HF39	125	125
Trichophyton equinum			
A	HF42	125	250
B	HM44	125	250
C	HF57	125	125

Table 8: Results of Commercially Standardized Antifungal Agents on Dermatophytes Isolates (Horses)

Drugs Samples	KCA	TER	NY	PB	AMB	ITC	AGF
Microsporum gyseum							
HM3	S(10mm)	S(28mm)	S(10mm)	R	R	R	R
HM8	S(10mm)	S(30mm)	S(11mm)	R	R	R	R
Microsporum audounii							
HM13	S(25mm)	S(35mm)	S(20mm)	S(10mm)	R	S(25mm)	R
HF50	S(11mm)	S(30mm)	S(18mm)	10(10mm)	R	S(20mm)	R
HF31	S(11mm)	S(28mm)	S(11mm)	R	R	R	R

Assessing the Antifungal Activities of Buchholzia Coriacea on Dermatophytes Isolated from Horses in Katsina State, Nigeria

© 2022 London Journals Press   Volume 22 | Issue 12 | Compilation 1.0   31

Trichophyton rubrum							
HM58	S(22mm)	S(33mm)	S(15mm)	S(13mm)	R	R	R
Trichophyton verrucossum							
HM39	S(16mm)	S(28mm)	R	R	R	R	R
HM45	S(18mm)	S(30mm)	R	R	R	R	R
Trichophyton equinum							
HM42	S(28mm)	S(40mm)	S(15mm)	S(10mm)	R	S(25mm)	R
HM44	S(25mm)	S(28mm)	S(10mm)	R	R	S(20mm)	R
HF57	S(26mm)	S(32mm)	S(13mm)	S(10mm)	R	S(22mm	R
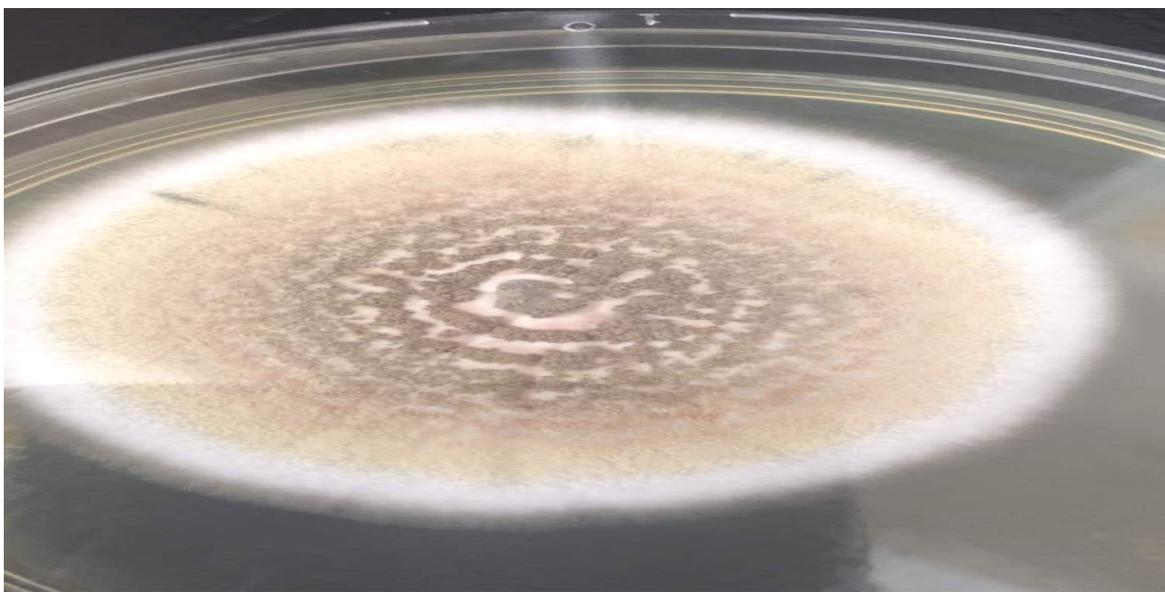
Plate I: A colony of *Microsporum gypseum* on PDA having dark to a cinnamon brown appearance with granular texture after 10 days growth at room temperature of 25° c
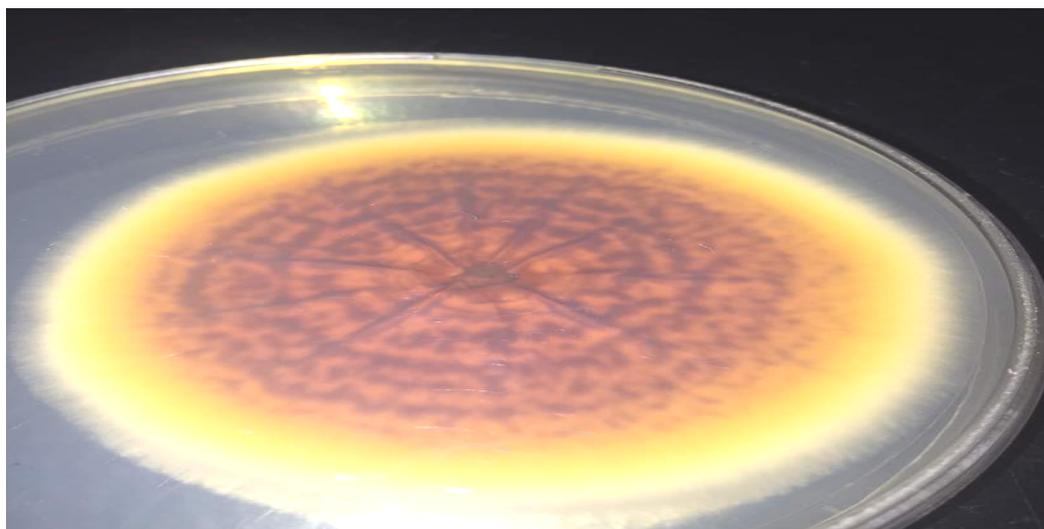
Plate II: The reverse side of *Microsporum gypseum* with slight yellow to red coloration

Assessing the Antifungal Activities of Buchholzia Coriacea on Dermatophytes Isolated from Horses in Katsina State, Nigeria

32 Volume 22 | Issue 12 | Compilation 1.0 © 2022 London Journals Press
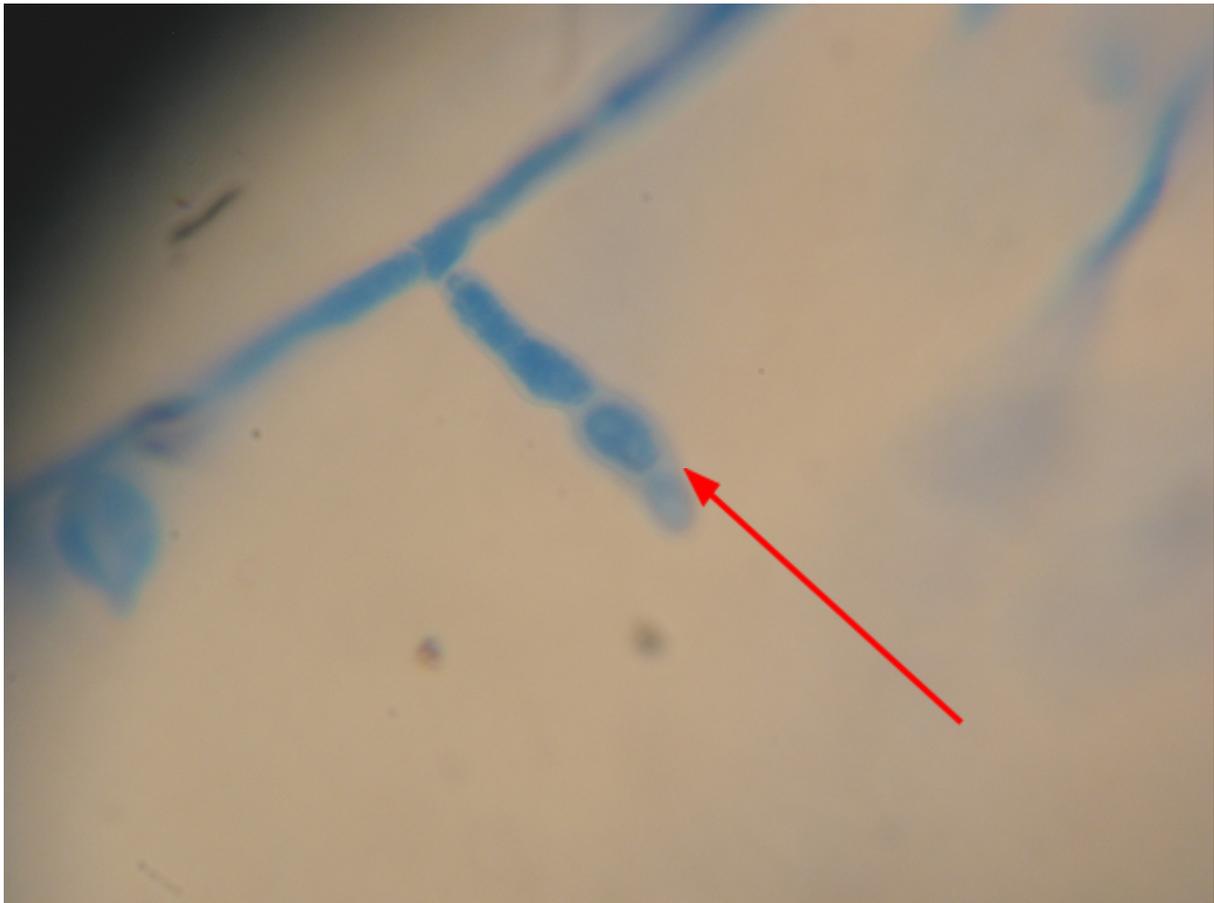
Plate III: Microscopy of *Microsporum gypseum* showing barrel-shaped macro conidia (x400) (LCB stain)

Plate IV: Colony of *Trichophyton verrucossum* having a cream coloured glabrous growth after 14 days growth on PDA at 25°c

Assessing the Antifungal Activities of Buchholzia Coriacea on Dermatophytes Isolated from Horses in Katsina State, Nigeria

© 2022 London Journals Press   Volume 22 | Issue 12 | Compilation 1.0   33
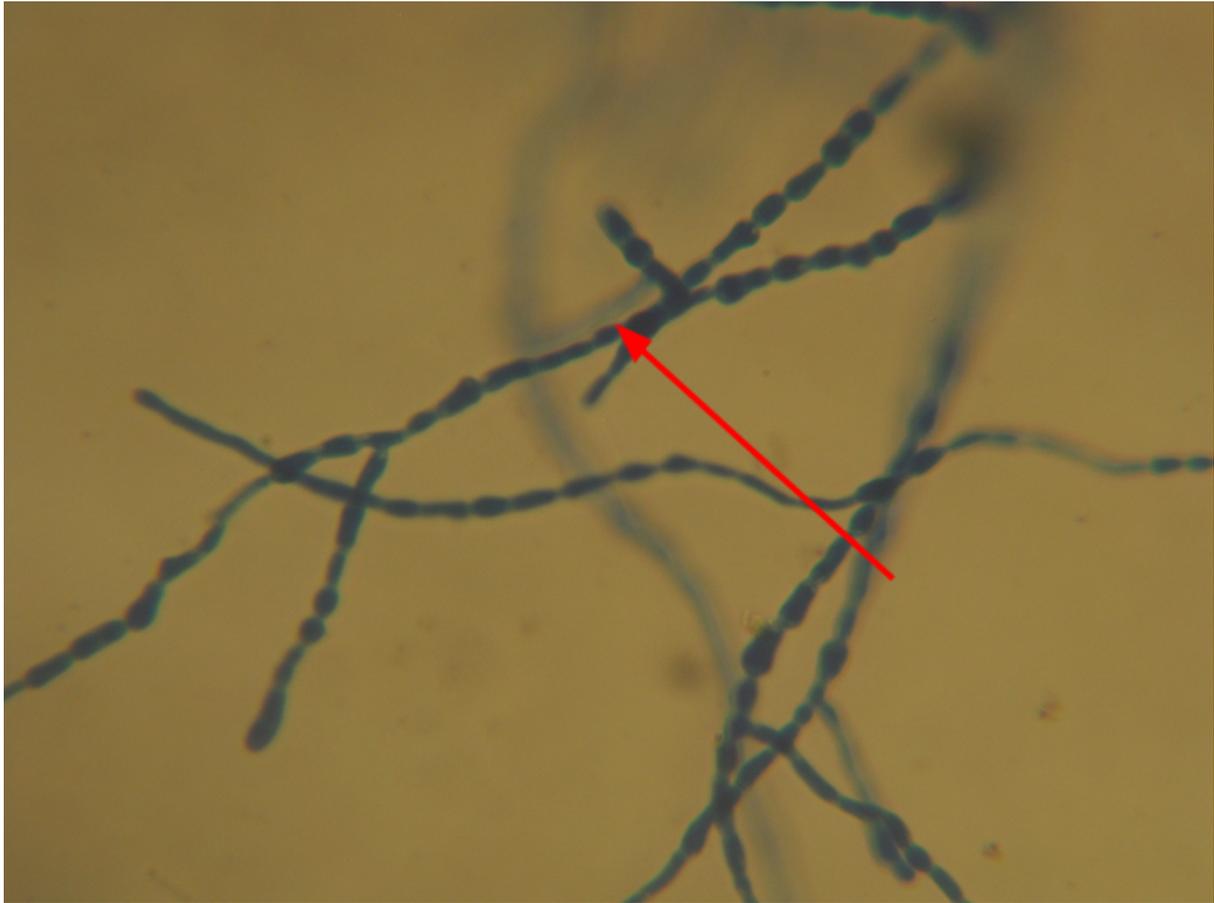
Plate V: Microscopy of *Trichophyton verrucossum* with a arrow indicating the Chlamydospores (x400) (LCB stain)
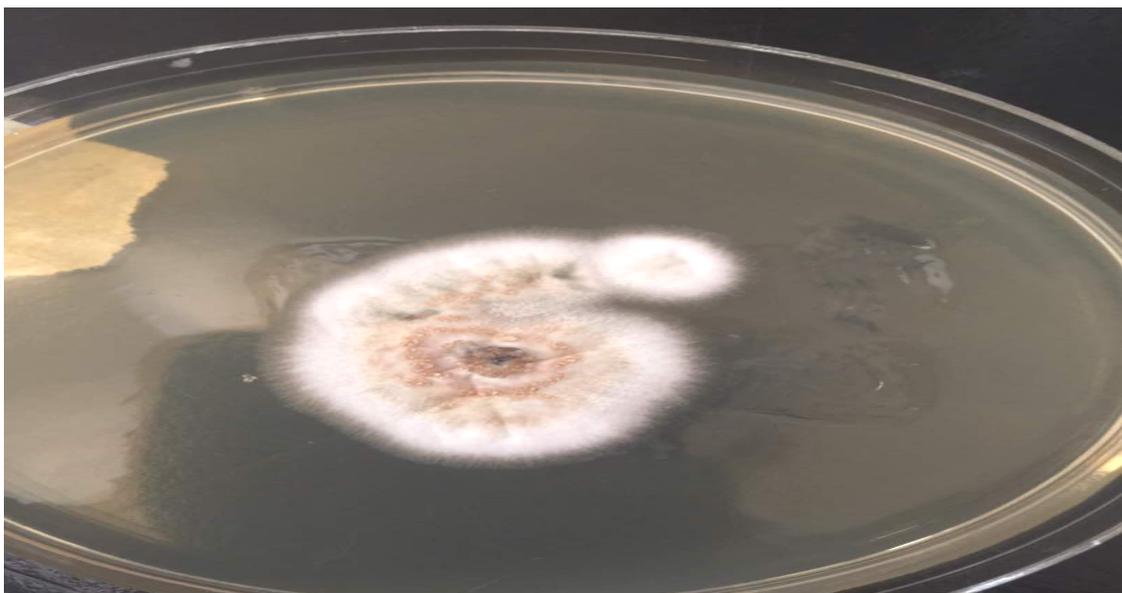
Plate VI: A colony of *Microsporum audouinii* on PDA exhibiting gray to white downy texture, after 14 days growth at room temperature of 25°c

Assessing the Antifungal Activities of Buchholzia Coriacea on Dermatophytes Isolated from Horses in Katsina State, Nigeria

34   Volume 22 | Issue 12 | Compilation 1.0   © 2022 London Journals Press
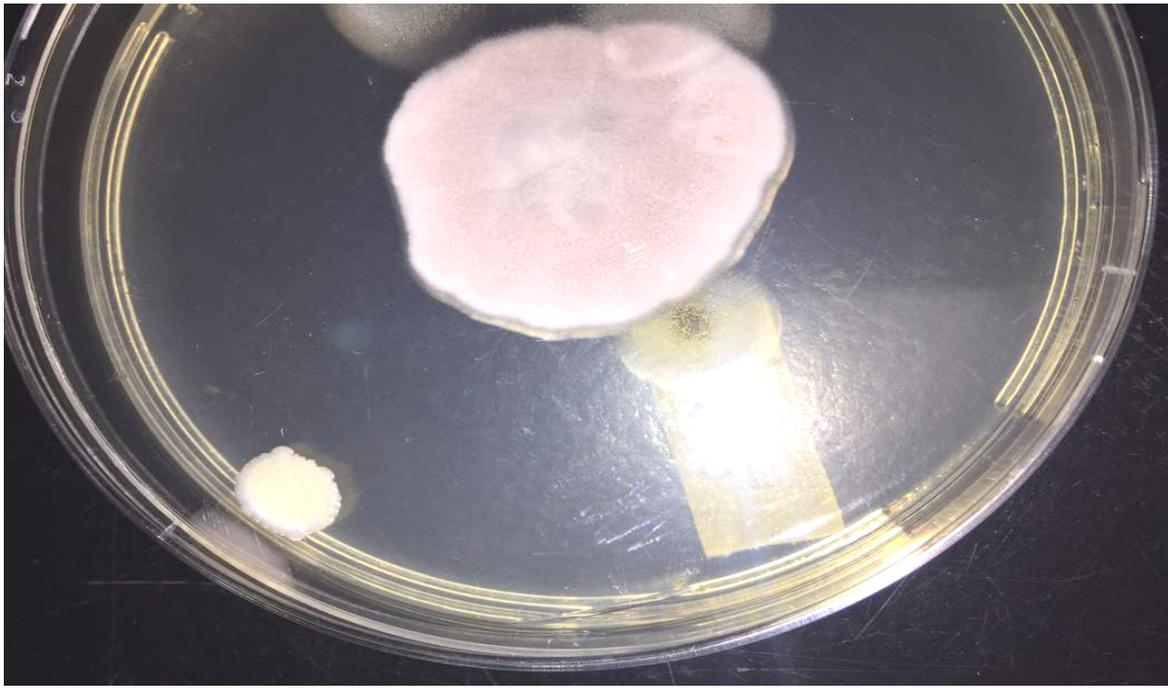
Plate VII: A colony of *Trichophyton equinum* on PDA with cream white to yellow appearance after 12 days growth

IV. DISCUSSION

Dermatophytes of the genera Microsporum and Trichophyton from horses were isolated and identified as a result of the investigation. The most frequent species were Trichophyton, which is consistent with the findings of Collise *et al.,* (2011), Nweze (2010), and Hassan (2011). This investigation confirmed the presence of three Trichophyton species (*T. equinum, T. rubrum, T. verrucosum*) and two Microsporum species (*M. gypseum, and M. audounii*) in the study area implicated in equine dermatophytoses. This is consistent with the writings of Nweze (2010) and *Popoola et al.,* (2006).

The highest isolated Trichophyton etiological agent was *Trichophyton equinum.* The works of Barros, (2007) and Kharna and Bharti, (2014), which noted that *T. equinum* is the most frequent isolated Dermatophytes species from horses and *T. verrucossum* from cattle, concur with this finding. The second-most isolated Dermatophyte in this investigation was *Microsporum audonii.* It is a fungus that infects animals that frequently come into contact with soil (Haria and Bryson, 1995). The location where the study was conducted may have contributed to the high abundance of this particular species.

One of the most typical ringworm causes in the globe is *Trichophyton rubrum*, which was isolated for this investigation. It is primarily blamed for nail and finger Dermatophytes infections (Seanego and Ndip, 2012). The most isolated were in the head and the back. All of the isolated *Trichophyton verrucosum* in this study came from horses' backs. The proximity of the cattle, horses, and donkeys may have contributed to the high number of positive cases discovered in horses.

This study has established a strong link between anatomical distribution and the isolated Dermatophytes. Horses' backs showed the highest distribution rate for Dermatophytes isolates, with Trichophyton having the most isolates. This is also in line with the OIE data from 2005, which suggested that the bulk of Dermatophytes lesions are seen on horses' backs that have come into contact with saddles. The age range from 6 to 10 years old saw the highest prevalence of Dermatophytes. This is explained by the fact that activities like sports and farm work are more common among people in this age group. Males

Assessing the Antifungal Activities of Buchholzia Coriacea on Dermatophytes Isolated from Horses in Katsina State, Nigeria

had a higher incidence of Dermatophytoses than females, according to the study.

Chi-square tests were used to analyze the link between the isolates and the test parameters, and the results revealed a significant difference between the distribution of the isolates and anatomical sites. In terms of the occurrence of the isolates, the anatomical sites are also distinct from one another. The p value of 0.061 at the 10% threshold of significance led to this conclusion. All of the isolates were subjected to the antifungal effects of the *Buchholzia coriacea* methanolic extract. *Trichophyton verrucossum* had MIC of 125 mg/ml and MFC of 250 mg/ml, indicating susceptibility to the extract. At MICs of 125 mg/ml and 250 mg/ml, *Microsporum gypseum* demonstrated susceptibility. The MICs and MFCs were the same for all other isolates.

Terbinafine results demonstrated the greatest level of effectiveness against all isolated species; supporting the claims made by Favre *et al.,* (2003) and Sitterle *et al.,* (2012) that terbinafine can be used to treat the majority of Dermatophytes infections in horses. Amphotericin B, one of the most widely used antifungal medications, was not effective against any of the isolates. This backed up the studies by Elewski (2000) that showed how amphotericin B was ineffective against dermatophytoses.

Against each isolate, Ketoconazole and Terbinafine demonstrated a high level of antifungal activity. The two medications that did not exhibit any antifungal action against the Dermatophytes isolated from the study area were Amphotericin B and Griseofulvin.

IV. CONCLUSION

This investigation was successful in proving *Buchholzia coriacea*'s methanolic extract's antifungal effectiveness. All of the isolates were susceptible to the *Buchholzia coriacea* methanolic extract's antifungal effects at various MICs and MFCs. The recommended medications include Terbinafine and Ketoconazole because they all shown antifungal efficacy against all isolates. The study was able to identify two Dermatophytes species; Trichophyton and

Microsporum in Nigeria's Katsina state, proving their presence there. It offers a base upon which subsequent study in the research area can be conducted.

REFERENCES

1. Barros, M. E. D. S., Santos, D. D. A., & Hamdan, J. S. (2007). Antifungal susceptibility testing of Trichophyton rubrum by E-test. *Archives of Dermatological Research*, *299*(2), 107–109.

2. Chermette, R., Ferreiro, L., & Guillot, J. (2008). Dermatophytoses in animals. *Mycopathologia*.

3. Collise, N., Anthony, J. A., Anna, M. C., & Roland, N. N. (2011). Crude Ethanolic Extracts of Garcinia kola Seeds Heckel (Guttiferae) Prolong the Lag Phase of Helicobacter pylori: Inhibitory and Bactericidal Potential. *Journal of Medicinal Food*, *14*(7–8), 822–827.

4. Degreef, H. (2008). Clinical forms of dermatophytosis (ringworm infection). *Mycopathologia*.

5. Elewski, B. E. (2000). *Tinea capitis*: a current perspective. *Journal of the American Academy of Dermatology*, *42*(1 Pt 1), 1-20-24.

6. Favre, B., Hofbauer, B., Hildering, K. S., & Ryder, N. S. (2003). Comparison of in vitro activities of 17 antifungal drugs against a panel of 20 dermatophytes by using a microdilution assay. *Journal of Clinical Microbiology*, *41*(10), 4817–4819.

7. Gupta, A. K., Chaudhry, M., & Elewski, B. (2003). *Tinea corporis*, *tinea cruris*, *tinea nigra*, and piedra. *Dermatologic Clinics*.

8. Hainer, B. (2003). Dermatophyte infections. *American Family Physician;*, *67*(1), 101–108.

9. Haria, M., & Bryson, H. M. (1995). Amorolfine. A review of its pharmacological properties and therapeutic potential in the treatment of onychomycosis and other superficial fungal infections. *Drugs*, *49*(1), 103–120.

10. Iwu, M. M., Igboko, O. A., Okunji, C. O., & Tempesta, M. S. (1990). Antidiabetic and aldose reductase activities of biflavanones of Garcinia kola. *Journal of Pharmacy and Pharmacology*, *42*(4), 290–292.

London Journal of Research in Science: Natural and Formal

Assessing the Antifungal Activities of Buchholzia Coriacea on Dermatophytes Isolated from Horses in Katsina State, Nigeria

36 | Volume 22 | Issue 12 | Compilation 1.0

© 2022 London Journals Press

11. Khanna, D., & Bharti, S. (2014). Luliconazole for the treatment of fungal infections: an evidence-based review. *Core Evidence, 9,* 113–124.

12. Mihali, C. V., Buruiana, A., Turcus, V., Covaci, A., & Ardelean, A. (2012). Comparative studies of morphology and ultrastructure in two common species of dermatophytes: Microsporum canis and Microsporum gypseum. *Annals of the Romanian Society for Cell Biology, 17*(1), 85–89.

13. Nweze, E. I. (2010). Dermatophytosis in West Africa- a review.pdf. *Pakistan Journal of Biological Sciences, 13*(13), 649–656.

14. Nweze, E. I., Ogbonna, C. C., & Okafor, J. I. (2007). In vitro susceptibility testing of dermatophytes isolated from pediatric cases in Nigeria against five antifungals. *Revista Do Instituto de Medicina Tropical de Sao Paulo, 49*(5), 293–295.

15. Penduka, D., Okoh, O. O., & Okoh, A. I. (2011). In-Vitro antagonistic characteristics of crude aqueous and methanolic extracts of *Garcinia kola* (Heckel) seeds against some Vibrio bacteria. *Molecules, 16*(4), 2754–2765.

16. Popoola, T. O. S., Ojo, D. A., & Alabi, R. O. (2006). Prevalence of dermatophytosis in junior secondary schoolchildren in Ogun State, Nigeria. *Mycoses, 49*(6), 499–503.

17. RIM. (1992). *Nigerian National Livestock Resource Survey.*

18. Rodwell, G. E. J., Bayles, C. L., Towersey, L., & Aly, R. (2008). The prevalence of dermatophyte infection in patients infected with human immunodeficiency virus. *International Journal of Dermatology, 47*(4), 339–343.

19. Rogers, B., Decottignies, a, Kolaczkowski, M., Carvajal, E., Balzi, E., & Goffeau, a. (2001). The pleitropic drug ABC transporters from *Saccharomyces cerevisiae. Journal of Molecular Microbiology and Biotechnology, 3,* 207–214.

20. Seanego, C. T., & Ndip, R. N. (2012). Identification and antibacterial evaluation of bioactive compounds from *Garcinia kola* (Heckel) seeds. *Molecules, 17*(6), 6569–6584.

21. Sitterle, E., Frealle, E., Foulet, F., Cabaret, O., Cremer, G., Guillot, J., … Botterel, F. (2012). Trichophyton bullosum: A new zoonotic dermatophyte species. *Medical Mycology, 50*(3), 305–309.

22. Warycha, M. A., Leger, M., Tzu, J., Kamino, H., & Stein, J. (2011). Deep dermatophytosis caused by Trichophyton rubrum. *Dermatology Online Journal, 17*(10), 21.

Assessing the Antifungal Activities of Buchholzia Coriacea on Dermatophytes Isolated from Horses in Katsina State, Nigeria

This page is intentionally left blank

London Journal of Research in Science: Natural and Formal

Assessing the Antifungal Activities of Buchholzia Coriacea on Dermatophytes Isolated from Horses in Katsina State, Nigeria

38 | Volume 22 | Issue 12 | Compilation 1.0

© 2022 London Journals Press

Conceptual Challenges of Quantum Field Theory in Technology

M.V. Takook

ABSTRACT

In classical theory, phenomena are defined by the model of particles or waves, aiming to explain reality with certainty. In quantum theory, the phenomena are described by a quantum state $|훼, 푥\rangle$, which explains the reality with uncertainty. Although in quantum theory, the reality is probabilistic, the quantum state $|훼, 푥\rangle$ can be determined with certainty due to the unitarity principle. The technology needs deterministic phenomena, and then quantum technology must be constructed based on this fundamental quantum state. The critical point in quantum technology is to build the deterministic phenomena from the quan- tum state $|훼, 푥\rangle$: this is the main argument in the present article. The realization of quantum technology comprises three steps: constructing an appropriate quantum state, obtaining its time evolution, and detecting it deterministically.

Keywords: quantum technology, quantum states, deterministic, uncertainty.

Classification: DDC Code: 530.12 LCC Code: QC174.12

Language: English

Conceptual Challenges of Quantum Field Theory in Technology

M.V. Takook

ABSTRACT

In classical theory, phenomena are defined by the model of particles or waves, aiming to explain reality with certainty. In quantum theory, the phenomena are described by a quantum state $|\alpha, t\rangle$, which explains the reality with uncertainty. Although in quantum theory, the reality is probabilistic, the quantum state $|\alpha, t\rangle$ can be determined with certainty due to the unitarity principle. The technology needs deterministic phenomena, and then quantum technology must be constructed based on this fundamental quantum state. The critical point in quantum technology is to build the deterministic phenomena from the quan - tum state $|\alpha, t\rangle$ this is the main argument in the present article. The realization of quantum technology comprises three steps: constructing an appropriate quantum state, obtaining its time evolution, and detecting it deterministically.

Keywords: quantum technology, quantum states, deterministic, uncertainty

I.   INTRODUCTION

To explain a physical system, the physicist constructs a theoretical model, and when the model cannot explain the experimental results, older models are replaced with new ones. In classical paradigm, the physical systems are usually described by particles, $x_i^\mu(\lambda)$, and or waves (epitomised by electromagnetic 4-potential field $A_\mu(t, \vec{x})$), which are immersed in space-time (*i.e.* the gravitational field $g_{\mu\nu}(t, \vec{x})$). λ is the particle path parameter in space-time. An elementary particle has intrinsic properties such as mass (m), electrical charge (q), spin (s), flavour (f) and colour (c), where the numerical values can be determined experimentally. The last three properties can be measured at the atomic and subatomic levels. These intrinsic properties are associated with four fundamental interactions in nature and play an important role in technology.

The complete information concerning the motion of a particle in general relativity is encoded in $x^\mu(\lambda)$ which can be found from the following equation [1, 2, 3]:

$$\frac{d^2 x^\mu}{d\lambda^2} + \Gamma^\mu_{\nu\rho} \frac{dx^\nu}{d\lambda} \frac{dx^\rho}{d\lambda} = F^\mu, \qquad (1.1)$$

where $\Gamma^\mu_{\nu\rho}$ are Christoffel symbols and F^μ is the force acting on the particle. Knowing the initial conditions (which can be obtained from observation) allows us to determine $\vec{x}(t)$ with certainty. All the properties of the particle, its velocity, acceleration, momentum, energy, etc., can be explicitly derived from $\vec{x}(t)$.

A stationary charged particle will produce an electric field. In contrast, a moving charged particle will create an electric current and a magnetic field, and an accelerated charged particle will create an electromagnetic field. The latter can be determined from the electromagnetic 4-potential field $A_\mu(t, \vec{x})$ which satisfies the following field equation in the flat Minkowski space-time [4]:

$$\partial_\nu \partial^\nu A_\mu(x) - (1 - l)\partial_\mu \partial \cdot A = j_\mu, \qquad (1.2)$$

where l is the Lagrange multiplier and j_μ is the 4-current density. Suppose we know the initial conditions of the 4-potential field at any given time. In that case, we will be able to find $A_\mu(t, \vec{x})$ at any later or earlier time by explicit calculation, which in turn enables us to find the electric and magnetic fields with certainty, *i.e.* $\vec{E}(t, \vec{x})$ and $\vec{B}(t, \vec{x})$). Thus, we can also determine all electromagnetic field information with certainty, such as energy distribution, momentum, angular momentum, etc.

In the theory of Einstein's general relativity, space-time is equivalent to the gravitational field and represented by the tensor potential field $g_{\mu\nu}(t, \vec{x})$, which is the solution of the Einstein field equation [1, 2, 3]:

$$R_{\mu\nu} - \frac{1}{2}Rg_{\mu\nu} + \Lambda g_{\mu\nu} = 8\pi G T_{\mu\nu}, \tag{1.3}$$

where $T_{\mu\nu}$ is the stress-energy tensor, $R_{\mu\nu}$ is the Ricci tensor, R is the scalar curvature, and Λ is the cosmological constant. If we have the initial conditions of the space-time, the metric $g_{\mu\nu}$ can be determined by the field equation (1.3). It is important to note that a tensor field describes space-time in general relativity. It can be imagined as a 4-dimensional curved hyper-surface immersed in a 5-dimensional flat Minkowski space-time.

According to the principles of classical theory, the solutions of the equation of motion, together with the boundary conditions (which can be obtained empirically), fully determine all natural phenomena or physical systems, and we can likewise understand them deterministically. The truth and reality of a physical system are equal, and both exist before the observation, which is the reality principle. The other important focus of the classical theory is that of locality, which forbids the simultaneous influence of one observer's observation on another's [5, 6].

II. THE QUANTUM PARADIGM

In quantum theory, the physical systems are described by a quantum state $|\alpha, t\rangle$, belonging to either the Hilbert space or the Fock space, depending on whether we are concerned with the first quantization or the second quantization (quantum field theory), respectively [6]. Therefore quantum technology must be constructed on the quantum state $|\alpha, t\rangle$.

In the flat Minkowski space-time, the quantum state $|\alpha, t\rangle$ is the solution of the following field equation:

$$i\hbar \frac{\partial}{\partial t}|\alpha, t\rangle = H|\alpha, t\rangle, \quad \text{or} \quad |\alpha, t\rangle = U(t, t_0; H)|\alpha, t_0\rangle, \tag{2.1}$$

where H is the Hamiltonian of the system and $U(t, t_0; H)$ is the time evolution operator. To obtain the explicit form of the quantum state $|\alpha, t\rangle$, we need to know the initial state $|\alpha, t_0\rangle$. Classically the initial state of the system is obtained from observations. Still, in quantum mechanics, the act of observation causes the state $|\alpha, t_0\rangle$ to collapse into the state $|\beta, t_0\rangle$. Evidently $|\beta, t_0\rangle$ is not the same as $|\alpha, t_0\rangle$ so that it is impossible for an observer to obtain and comprehend the quantum state $|\alpha, t\rangle$. Accordingly, how can we construct quantum technology? By choosing the quantum state $|\beta, t_0\rangle$ as the initial state after observation, quantum technology can be built, which will be clarified in this article.

Quantum technology has two different periods of progress. The first was constructed based on the probability amplitude and the second on the quantum state $|\alpha, t\rangle$, which will be discussed in the following sections.

2.1. **The first quantum industrial revolution.** The first quantum industrial revolution began with observing electrons' wave properties, which came from quantizing a particle. It is the so-called first quantization in which a wave function describes a particle, $\psi_\alpha(t, \vec{x})$, *i.e.* a classical field. However, the observed properties of the particle are explained with a probability density function in space $|\psi_\alpha(t, \vec{x})|^2 = |\langle \vec{x}|\alpha, t\rangle|^2$. Thus a phenomenon or a particle is described by the probability amplitude $\langle \vec{x}|\alpha, t\rangle$. From such a perspective, the quantum state $|\alpha, t\rangle$ is merely an auxiliary mathematical object immersed in Hilbert space. Despite the probability density function immersed in space-time, in this case, the Hilbert space is a purely mathematical subject.

Although the first quantization successfully explains the structure of atoms and predicts many fundamental particles, it suffers from many practical and philosophical problems, such as the creation and annihilation of particles and particle-wave duality. These problems are pretty solved in second quantization or quantum field theory.

The first quantization leads to the first quantum technology revolution. Technologies generated by the first quantization are electron microscope, nuclear power, Laser, transistors and semiconductor devices, and other devices such as MRI devices.

2.2. **The second quantum industrial revolution.** The second quantum industrial revolution was begun by observing the single photon (or particle properties of radiation field), and wave properties of the single-photon by Aspect et al. [7, 8]. Their observations were based on quantum field theory (QFT), also called second quantization. In the QFT model, a phenomenon or a physical system is described by a quantum state $|\alpha, t\rangle$, which is immersed in the Fock space. In this case, the Fock space is not a purely mathematical subject and it has observable physical properties.

The construction procedure of the quantum technology in this case may be performed in three steps: 1- the construction of a suitable quantum state $|\beta, t_0\rangle$, 2- obtaining its time evolution under the influence of the new interaction Hamiltonian H_n: $|\beta, t\rangle = U(t, t_0; H_n)|\beta, t_0\rangle$, and 3- its detection or observation, $|\beta, t\rangle \longrightarrow |\gamma\rangle$. This process will be briefly discussed in this article.

A class of devices actively create, manipulate, and read out quantum states of a system, often using the quantum effects of superposition and entanglement. The second quantum technologies revolution is constructed on the quantum state $|\alpha, t\rangle$ by applying its quantum properties such as entanglement and superposition. This model results in quantum technology such as quantum computing, sensors, cryptography, simulation, quantum metrology, quantum imaging, high-power fiber laser, etc.

III. NON-RELATIVISTIC CASE

In this section, we briefly recall the Hilbert space $\mathscr{H}^{(1)}$ and quantum state $|\alpha, t\rangle$ of a free particle and a simple harmonic oscillator in the non-relativistic quantum mechanics, which is essential for understanding the quantum field theory and then quantum technology. In quantum mechanics, an observable is presented by a hermitian operator, which is defined as a mapping from the Hilbert space on itself:

$$\text{Operators}: \ \mathscr{H}^{(1)} \longrightarrow \mathscr{H}^{(1)}, \quad and \ \ |\alpha, t\rangle \in \mathscr{H}^{(1)}.$$

In quantum mechanics, the Hilbert space plays the same role as the space-time in classical theory. Like space-time, the Hilbert space of a physical system is unique, but one can define the different basis for the Hilbert space similarly to the various coordinate systems in space-time.

3.1. **Free particle.** The Hamiltonian of a free particle is $H = \frac{p^2}{2m}$. Two important basis of the Hilbert space are $|\vec{k}\rangle$ and $|k, l, m_l\rangle$, which result in the plane wave ($\langle \vec{x} | \vec{k} \rangle \propto e^{-i\vec{k}\cdot\vec{x}}$) and spherical wave, respectively. The identity operator on these bases are:

$$I_{\vec{k}} = \int d^3k \ |\vec{k}\rangle\langle\vec{k}|, \quad I_{klm_l} = \int dk \sum_{l,m_l} |k, l, m_l\rangle\langle k, l, m_l|.$$

The quantum state can be written as:

$$|\alpha, t\rangle = \int d^3k \ |\vec{k}\rangle\langle\vec{k}|\alpha, t\rangle = \int dk \sum_{l,m_l} |k, l, m_l\rangle\langle k, l, m_l|\alpha, t\rangle = e^{-\frac{i}{\hbar}H(t-t_0)}|\alpha, t_0\rangle. \tag{3.1}$$

The sum or integral over the basis is a superposition. The outcome of a measurement depends on the initial state ($|\alpha, t_0\rangle$) and the Hamiltonian of the detector (H_d). If the initial state is one of the basis of Hilbert space, the time evolution only changes its phase, $|\alpha, t\rangle = e^{-i\frac{\vec{k}\cdot\vec{k}\hbar}{2m}t}|\vec{k}\rangle$ and if we have $[H, H_d] = 0$, the observed state is not a superposition of states.

3.2. **Simple harmonic oscillator.** The Hamiltonian of a simple harmonic oscillator is:

$$H = \frac{p^2}{2m} + \frac{1}{2}m\omega^2 x^2 = \left(N + \frac{1}{2}\right)\hbar\omega, \quad N = a^\dagger a, \tag{3.2}$$

where a is the annihilation operator and N is the Number operator. In this case, three important bases for the Hilbert space, which we know them, are number states, coherent states, and squeezed states. The number states are the eigenstates of the number operator $N|n\rangle = n|n\rangle$. We have

$$a|0\rangle = 0, \quad a|n\rangle = \sqrt{n}|n-1\rangle, \quad a^\dagger|n\rangle = \sqrt{n+1}|n+1\rangle, \quad |n\rangle = \frac{(a^\dagger)^n}{\sqrt{n!}}|0\rangle. \tag{3.3}$$

$|n\rangle$ is a complete orthonormal basis:

$$I_n = \sum_{n=0}^{\infty} |n\rangle\langle n|, \quad n = 0, 1, 2, \cdots, \quad \langle n|m\rangle = \delta_{nm}. \tag{3.4}$$

The variance or the mean square deviation of x and p are:

$$\langle n|(\Delta x)^2|n\rangle = \left(n + \frac{1}{2}\right)\frac{\hbar m}{\omega}, \quad \langle n|(\Delta p)^2|n\rangle = \left(n + \frac{1}{2}\right)\frac{\hbar\omega}{m}. \tag{3.5}$$

They are minimum only for the ground state $n = 0$.

The coherent states are the eigenstates of the annihilation operator $a|z\rangle = z|z\rangle$, $z \in C$ [9, 10]. We have

$$|z\rangle = D(z)|0\rangle = e^{za^\dagger - z^* a}|0\rangle = e^{-\frac{zz^*}{2}}\sum_n \frac{z^n}{\sqrt{n!}}|n\rangle, \quad D(z)|z'\rangle = e^{\frac{zz'^* - z'z^*}{2}}|z + z'\rangle, \tag{3.6}$$

where $D(z)$ is the displacement operator. The average of number operator and the time evolution of the coherent state are:

$$|z(t)\rangle = U(t)|z\rangle = e^{-i\frac{\omega t}{2}}e^{-i\frac{\omega t}{2}N}|z\rangle = e^{-i\frac{\omega t}{2}}|e^{-i\frac{\omega t}{2}}z\rangle, \quad \langle z|N|z\rangle = |z|^2. \tag{3.7}$$

Then in the time evolution, the mean square deviation of x and p are constant and minimum:

$$\langle z(t)|(\Delta x)^2|z(t)\rangle = \frac{\hbar m}{2\omega}, \quad \langle z(t)|(\Delta p)^2|z(t)\rangle = \frac{\hbar\omega}{2m}. \tag{3.8}$$

It is an exciting result, which is very important for quantum technology. The Laser produces the coherent state of electromagnetic field [11], and for signal and image processing, the coherent state may be used [12, 9, 10]. The coherent state may be used for signal, and image processing in MRI instead of Fourier transformation for minimum error [13].

If we define an annihilation operator, which is rotated in plane $(a, a^\dagger)$, such as:

$$a_s \equiv \cos\beta\, a + \sin\beta\, a^\dagger, \tag{3.9}$$

the variance of x and p are the functions of β as:

$$\begin{cases} \Delta x_s = \Delta x \cos\beta + \Delta p \sin\beta, \\ \Delta p_s = -\Delta x \sin\beta + \Delta p \cos\beta. \end{cases} \tag{3.10}$$

The variance or the mean square deviation of x_s or p_s can become less than the coherent state for some value of β. This property of the squeezed states is used to detect the gravitational wave in the LIGO experiment [14]. The squeezed state is defined as the eigenstates of the annihilation operator a_s:

$$a_s|v, z\rangle = f(v, z)|v, z\rangle, \quad v \equiv e^{i\beta}. \tag{3.11}$$

It can be written as:

$$|v, z\rangle = S(v)D(z)|0\rangle, \quad S(v) = e^{\frac{1}{2}(v^* a^2 - v a^{\dagger 2})}. \tag{3.12}$$

Squeezed states can be experimentally produced by forcing coherent states to propagate through a non-linear medium, which reproduces the effect of the non-linearity of the Hamiltonian [15],

$$|v, z\rangle \equiv e^{-iH_I t/\hbar}|z\rangle, \quad H_I = \frac{i\hbar}{2t}\left(v^* a^2 - v a^{\dagger 2}\right), \tag{3.13}$$

This property is essential for quantum tomography and has many applications in Lithography and medicine. Nano-lithography or advanced lithography is vastly used in producing nanoelectronic devices [16, 17]. Squeezed states have much application in detecting and photographing [14] and making electronic components [18, 19]. Squeezed states can also be used in MRI for best imaging resolution [20].

Different bases of Hilbert space can be used in quantum technology, such as quantum computation, quantum tomography, high-power fiber Laser, etc. [21, 22]. The construction of solid-state Lasers and high-power fiber lasers has many applications in industry, military, oil industry, etc. Lasers also have a wide range of medical applications, from imaging and diagnosis to treatment and surgery [11, 23].

If we assume that the Hamiltonian is time-independent and the initial state is one of the Hamiltonian eigenstates $|\alpha, t_0\rangle = |m\rangle$ $(H|m\rangle = E_m|m\rangle)$, during the time evolution only the phase of the quantum state is changed:

$$|\alpha, t\rangle = e^{-iE_m(t-t_0)/\hbar}|m\rangle,$$

whereas if the initial state is a superposition of different Hamiltonian eigenstates, $|\alpha, t_0\rangle = \sum_n c_n|n\rangle$, then the quantum state of the physical system is a complex superposition of states:

$$|\alpha, t\rangle = \sum_n e^{-iE_n(t-t_0)/\hbar}c_n|n\rangle.$$

A measurement of the physical system can be interpreted as an interaction with the system, and then one can define a new system that includes the measuring apparatus. We do this by introducing the perturbed Hamiltonian $H_T = H + H_d$. If $[H, H_d] = 0$ and the initial state is a single state, then the quantum state of the physical system is also a single state, which may be interpreted as a particle in quantum field theory. In all other cases, the quantum state of the physical system would be a superposition of states, which may also be interpreted as the wave function. Through this short presentation, one can better understand the quantum field theory.

IV.   QUANTUM FIELD THEORY

In quantum field theory, H in equation (2.1) is the Hamiltonian of the relativistic fields, and the quantum state $|\alpha, t\rangle$ is immersed in Fock space. The classical Hamiltonian of the free field can be extracted from the field equation (Klein-Gordon equation, Dirac equation, Maxwell's equations, etc.). For the interaction fields, the Hamiltonian can be calculated from the gauge theory [24]. One of the essential parts of quantum technology is constructing the interaction Hamiltonian.

4.1. **Fock space.** Fock space is constructed by the relativistic one-particle Hilbert space as:

$$\mathcal{F}(\mathcal{H}) = \left\{C, \mathcal{H}^{(1)}, \mathcal{H}^{(2)}, \cdots, \mathcal{H}^{(n)}, \cdots\right\}, \quad |\alpha, t\rangle \in \mathcal{F}, \tag{4.1}$$

where C is vacuum state, $\mathcal{H}^{(1)}$ is one-particle states and $\mathcal{H}^{(n)}$ is n-particles states. n-particles states is constructed by tensor product of one-particle ststes (for bosons a symmetry product, $\mathcal{H}^{(2)} = S\mathcal{H}^{(1)} \otimes \mathcal{H}^{(1)}$ and for fermions an anti-symmetric products, $\mathcal{H}^{(2)} = A\mathcal{H}^{(1)} \otimes \mathcal{H}^{(1)}$).

The kinematical group of the Minkowski space-time is the Poincare group. By using the Lie algebra of this group, the one-particle states and unitary irreducible representation of this group can be constructed as [25]:

$$U^{(m,s)}(\Lambda, a)\,|k^{\mu}, m_s; s, m\rangle = e^{-ia\cdot\Lambda k}\sqrt{\frac{(\Lambda k)^0}{k^0}}\sum_{m'_s}D^{(s)}_{m'_s m_s}(\Lambda, k)|(\Lambda k)^{\mu}, m'_s; s, m\rangle, \qquad (4.2)$$

where $\Lambda \in SO(1,3)$, $a^{\mu} \in R^4$ and $D^{(s)}_{m'_s m_s}(\Lambda, k)$ is a group representation of $SU(2)$. $k^{\mu} = (k^0, \vec{k})$ is the four-vector of energy-momentum. m is mass, s is spin, and the one-particle state is:

$$|k^{\mu}, m_s; s, m\rangle \equiv |1_k\rangle \in \mathscr{H}^{(s,m)}_{k,m_s} \equiv \mathscr{H}^{(1)}, \quad (k^0)^2 - (\vec{k}\cdot\vec{k}) = m^2 c^4/\hbar^2, \quad -s \le m_s \le s. \qquad (4.3)$$

The identity operator on the Fock space is:

$$I_F = \left(|0\rangle\langle 0| \oplus \int \tilde{d}k |1_k\rangle\langle 1_k| \oplus \int \tilde{d}k_1 \tilde{d}k_2 |1_{k_1}, 1_{k_2}\rangle\langle 1_{k_1}, 1_{k_2}| \oplus \cdots \right), \qquad (4.4)$$

where $\oplus$ is tensorial sum, $|0\rangle$ is vacuum state, $\tilde{d}k$ is Lorentz invariant measure and $|1_k\rangle$ is the one-particle states. The field operator is defined as a mapping from the Fock space on itself:

$$\text{Field Operators}: \; \mathscr{F}(\mathscr{H}) \longrightarrow \mathscr{F}(\mathscr{H}).$$

In quantum field theory, from the equations (4.2) and (4.4), one can see that there is two sum or integral, one overall possibility states in one-particle Hilbert space similar to the first quantization and the other general possibility states in Fock space. Therefore, the creation and annihilation of a particle can be explicitly explained, which is the most crucial problem of the first quantization. In this model, the physical systems are equivalent with the quantum state $|\alpha, t\rangle \in \mathscr{F}$, and we have two statistics over observations: one over Hilbert space and the other on Fock space, which is complexly intertwined [26, 27]. This complexity must be well manipulated in quantum technology, an important theoretical and experimental research goal.

In quantum field theory, the particle-wave duality is meaningless. The observer can observe different aspects of the physical system from the particle and classical waves, which will be discussed in the following subsection for the electromagnetic field (for simplicity).

4.2. **Electromagnetic field.** For quantization of the electromagnetic field, we must begin with the Hamiltonian of this field. The Hamiltonian of the electromagnetic free field with two physical polarization states is [28]:

$$H = \int d^3x \, \frac{1}{2}\left(E^2 - B^2\right) = \int \tilde{d}k \sum_{m_s=1,2} \hbar\omega_k\left[a^{(m_s)\dagger}(k)a^{(m_s)}(k) + \frac{1}{2}\right], \qquad (4.5)$$

where m_s is the polarization of the electromagnetic field or photon's spin direction, this Hamiltonian is constructed from an infinite number of the simple harmonic oscillator (3.2). Like a harmonic oscillator, one can define the number state as the number of photons. The particle number operator is defined as: $N(k, m_s) = a^{(m_s)\dagger}(k)a^{m_s}(k)$, which commute with the Hamiltonian (4.5), $[H, N(k, m_s)] = 0$. The electromagnetic field's coherent and squeezed states can be introduced, similar to the harmonic oscillator. In this case, the Laser produces

coherent states. Squeezed states can be experimentally produced by forcing coherent states to propagate through a non-linear medium.

Hence, within quantum field theory, the observation of what we usually call particles (in this case photons) or waves depends on the initial state $|\alpha, t_0\rangle$ and the Hamiltonian of the detector H_d as well. If the initial state is one of the number operator's eigenstates, then the physical system's quantum state contains a definite number of particles or quanta. In this case, we can observe the photon if $[H, H_d] = 0$. With a single photon, if $[H, H_d] \neq 0$, the interference is observed or the wave properties of the photon. It is interesting to note that in the number states, the concept of particles or quanta exists but the number of the particles is dependent on the detector energy, which manifests the fluctuation in the Fock space.

If the initial state is a superposition of the particle number operator's eigenstates, the physical system's quantum state ($|\alpha, t\rangle$) is a superposition of states, and the particles picture is inappropriate. One can only speak of the average number of photons or particles. We see that the particle-wave duality conundrum, well-known in ordinary quantum mechanics [5], disappears in the framework of the quantum field theory as the fundamental concept in quantum field theory is the quantum state $|\alpha, t\rangle$. Expressing this concept in entangled states shatters classical physics' naive realism and locality. When a quantum field exists (for example, electron field, electromagnetic field, etc.), the corresponding quantum state $|\alpha, t\rangle$ also exists.

The reality observed by the observer depends on the apparatus of the observer, and reality observation is probabilistic, but the quantum state $|\alpha, t\rangle$ is deterministic due to the unitarity principle ($UU^\dagger = 1$):

$$|\alpha, t\rangle = U(t, t_0)|\alpha, t_0\rangle \implies \text{Observations} \implies |\beta, t_0\rangle \equiv \begin{cases} \text{Particles,} \\ \text{Classical waves,} \\ \text{Number state,} \\ \text{Coherent states,} \\ \text{Squeezed states,} \\ \cdots . \end{cases} \quad (4.6)$$

In the model of quantum theory, the quantum state $|\alpha, t\rangle$ may be considered the truth of the physical system, which is inaccessible to the observer, and the quantum state $|\beta, t_0\rangle$ as its reality. t_0 is the time of the observation. From the principles of quantum theory, one cannot obtain and comprehend the quantum state $|\alpha, t\rangle$ because we need the initial state for calculating $|\alpha, t\rangle$ and the observation for perceiving the physical system. However, after the observation, due to the collapse of the quantum state $|\alpha, t\rangle$, we obtained a new quantum state, and also the act of observation caused the state $|\alpha, t_0\rangle$ to collapse into the state $|\beta, t_0\rangle$. This new quantum state $|\beta, t_0\rangle$ is understandable for the observer because of observation.

Under the evolution of the new interaction H_n on the quantum states $|\beta, t_0\rangle$, due to the unitarity principle, one can obtain the time evolution of this quantum states $|\beta, t\rangle$ exactly or deterministically:

$$|\beta, t\rangle = U(t, t_0; H_n)|\beta, t_0\rangle, \quad UU^\dagger = 1 = U^\dagger U. \quad (4.7)$$

The critical point in quantum engineering or technology lies here. For the construction of the technology, we need a deterministic physical state, which now exists, $|\beta, t\rangle$. Therefore the process of quantum technology can be divided into three steps. The first step is constructing the quantum states $|\beta, t_0\rangle$, which requires high precision. Then we must obtain the best interaction Hamiltonian H_n in the atomic and subatomic levels. This step is

the most complicated part of quantum engineering, which requires collaboration between the different branches of engineering and physics. The final step is to detect the quantum state $|\beta, t\rangle$, which is also a complex problem. The final stage is also a probabilistic process. Using the entangled state, one can manipulate the other part of the entangling state for use in the quantum computer, which is an art of the experimentalist. The quantum computation (quantum algorithm), quantum information processing, quantum cryptography, quantum radar, quantum tomography, and quantum teleportation are based on quantum entanglement [29, 30, 31, 32, 33]. The IC programming must be done at the quantum level.

V. QUANTUM TECHNOLOGY

The classical technology is based on the intrinsic properties of electrical charge, and mass of the particles [34]. In quantum technology, the other inherent properties such as spin, flavor, and color may play a similar role. Still, due to the limitations of contemporary technology, spin only appears in quantum technology.

Before constructing quantum technology, we must accept that a physical system is equivalent to a quantum state, physical system $\equiv |\alpha, t\rangle$, which can be calculated deterministically using the quantum theory principles, unitarity principle. In the last decade, considerable advances have been achieved concerning the theoretical understanding, technical fabrication, and experimental characterization of the quantum state, $|\alpha, t\rangle$.

From the principles of quantum theory, we know that observation causes the collapse of the quantum state to a new quantum state, $|\beta, t_0\rangle$, which is a probabilistic process. The construction of quantum state $|\beta, t_0\rangle$, its time evolutions, and finally, its detection is an essential procedure of quantum technology. Therefore these procedures can be divided into three steps, briefly discussed in the following subsections.

5.1. **Quantum–state reconstruction.** Quantum technology is based on the construction of the quantum state, which generally uses the magnetic or spin properties of matter and electromagnetic field [35, 36, 37, 38]. The construction of quantum states of photons, phonons, and electric charge particles are vastly studied in the different disciplines of quantum engineering, such as photonics, solid-state physics, and plasma physics. We briefly recall two important experiments, which have been extensively used in technology for the reconstruction of the quantum states for charge spin $= \frac{\hbar}{2}$ particles and photons (spin $= 1\hbar$). The first one is the Stern-Gerlach experiment. In the original investigation, silver atoms were sent through a spatially varying magnetic field in the z direction, and the particles with non-zero magnetic moments were deflected in two branches. The spin quantum state of the particles is a superposition of the spin up and down in the z direction:

$$|\alpha, t\rangle = c_1 |z, +\rangle + c_2 |z, -\rangle. \tag{5.1}$$

The meaning of this superposition is not clear to our perception. After blocking $-z$ direction, which is equivalent with an observation or interaction, the quantum state collapse to the new quantum state $|\beta, t_0\rangle = |z, +\rangle$. Now, this quantum state can be undergone with a new interaction Hamiltonian, which will be discussed in the following subsection, and is obtained as its time evolution:

$$|\beta, t\rangle = U(t, t_0; H_n)|\beta, t_0\rangle = U(t, t_0; H_n)|z, +\rangle. \tag{5.2}$$

Because of the unitarity principle, we have explicitly the quantum state $|\beta, t\rangle$.

Conceptual Challenges of Quantum Field Theory in Technology

The second one is the Aspect et al. experiment [7, 8]. They produce polarization entangled photon-pair source, where the quantum state is:

$$|\alpha, t\rangle = \frac{1}{\sqrt{2}} \left[\, |H_1, H_2\rangle - |V_1, V_2\rangle \right]. \tag{5.3}$$

$H(V)$ is horizontal (vertical) polarization. After observing one photon, a single photon (another photon) generate with the specific polarization:

$$|\beta, t_0\rangle = |H\rangle, \quad \text{or} \quad |\beta, t_0\rangle = |V\rangle. \tag{5.4}$$

It is interesting to note that with the single-photon, the observer can observe the wave properties of the single-photon if the Hamiltonian of the detector cannot commute with the photon number operator, $[H_d, N] \neq 0$.

The production of quantum states is an experimental art and is precious in quantum technology. The Laser produces a coherent state. The squeezed states may be generated by forcing coherent states to propagate through a non-linear medium. The production of squeezed states can be extended to the case of condensed matter physics by replacing photons with phonons. Applying coherent and squeezed states in quantum engineering is vast and needs careful study.

5.2. **Interaction Hamiltonian.** The interactions used in technology may be divided into three types: charge particles-charge particles, charge particles-photons, and photons-photons. The first two interactions exist in classical theory, and they can also be explained in the first quantization and formulated by the gauge theory, following classical field Lagrangian density:

$$\mathscr{L}_c = -\frac{1}{2}\partial_\mu A_\nu \left(\partial^\mu A^\nu - \partial^\nu A^\mu\right) + \frac{1}{2}l\left(\partial \cdot A\right)^2 + \sum_n \bar{\psi}_n \left(i\gamma^\mu D_\mu^n - m_n\right)\psi_n, \tag{5.5}$$

where $D_\mu = \partial_\mu + iq_n A_\mu$ is the gauge covariant derivative, ψ_n is the particle-wave function, and n is defined as the type of the particles. $l \neq 0$ is an arbitrary constant. In this matter, n is a huge number, and it is also necessary to use the statistical mechanics [26, 27]. The photons-photons interactions can only be explained in the quantum field theory, where the effective Lagrangian density (effective potential) can be obtained by the loop-expansion approximation [24]:

$$\mathscr{L} = \mathscr{L}_c + \hbar\mathscr{L}^{(1)} + \hbar^2\mathscr{L}^{(2)} + \cdots . \tag{5.6}$$

Then the interaction Hamiltonian can be calculated theoretically by the equation (5.6).

Since calculating the effective potential is difficult for experimental researchers, the interaction Hamiltonian is usually obtained by trial and error. Therefore the most challenging problem in quantum engineering is to design the interaction Hamiltonian between the quantum state and matter or quantum field experimentally, which needs cooperation between the various discipline of physics and engineering. The interactions are generally based on field-matter properties: electric charge, spin, magnetic moment, and electric moment. In the interaction between the photons-photons and photons-matter, the non-linear optics and quantum optics play an essential role. In the magnetic properties of matter, matter's superconductivity and semiconductor properties are pretty important. If other materials are provided to it to form interfaces, remarkable devices can be made to control quantum states.

Researchers have coupled the monolayer form of carbon known as graphene with thin layers of magnetic materials like cobalt and nickel, producing the sort of exotic behaviors in

electrons that could be useful for next-generation computing applications. The interaction of graphene with magnetic materials affects the spin property of electrons. It has been studied as a route for driving low-energy, high-speed computer memory, and logic. The use of graphene may represent a revolutionary advance. Graphene is ultra-thin and lightweight, with very high electrical conductivity. Researchers are now working to form the graphene-magnetic multilayer material on an insulator or semiconductor to bring it closer to potential applications.

The nanoscale crystals, photonic crystals, and growing anisotropic crystals at the nanoscale have much application in nanoelectronic devices [39, 40]. The revolution has been taking place in the field of electronics with the development of nano transistors, quantum dots, quantum wires, and quantum wells [41, 19, 18]. The subjects such as nano-meter CMOS IC, circuit design IC and circuit design CPU are considered in this domain [42, 43]. Recently the researchers tried to use Plasmons [44, 45] and microwave circulator [44], which are based on quantum anomalous Hall effect [46, 47, 48], since they may support electrical currents that flow without resistance [44].

5.3. **Observation or detection.** In quantum theory, observation causes the collapse of the quantum state, which is probabilistic. However, for engineering technology, we need a deterministic result. This goal is achieved by using the entangled states. Entanglement will be used extensively as a powerful computational resource in quantum information processing and quantum computation. In the entangled two qubits state, the measurement of the first qubit affects the outcome of the measurement on the second qubit, which shows that the initial state is entangled. In other words, there exists a strong correlation between the two qubits. This correlation may be used for information processing. Suppose the register is set to an initial fiducial state, for example, $|\beta, t_0\rangle$. A unitary matrix $U(t, t_0)$ is designed to represent an algorithm we want to execute. Operation of U on $|\beta, t_0\rangle$ yields the output state $|\beta, t\rangle = U(t, t_0)|\beta, t_0\rangle$. Information is extracted from $|\beta, t\rangle$ by appropriate measurements [29]. For the homodyne detection and quantum state reconstruction, see [49] and references in it.

Some important entangled states are the Bell state, Greenberger-Horne-Zeilinger state (GHZ), W state (three-qubit state), and EPR state. An eight-qubit entangled state has been realized with an ion trap. The ion trap is one of the candidates for a scalable quantum computer [50]. Jaksch et al. proposed a method to prepare neutral-atom entangled states and Bell-like states, to be more specific, by controlling atom-atom collision time [51].

VI. CONCLUTION

The most important concept in the quantum theory is the quantum state $|\alpha, t\rangle$, which is modelled a phenomenon, *i.e.* physical system $\equiv |\alpha, t\rangle$. The reality, which is an observer-dependent quantity, is the collapse of a quantum state. From the general covariance, all observers are equivalence. Therefore, no one can claim that he has come to the truth because they have come to reality, and the truth is an illusion for the observer. In quantum theory, the truth of a natural phenomenon is a quantum state $|\alpha, t\rangle$, which is not accessible to the observer, and the reality is a specific collapse of the quantum state, *i.e.* $|\beta, t_0\rangle$, which is perceivable for the observer.

On the other part, technology needs deterministic phenomena. In this paper, we discussed how one could construct a quantum state, obtain its time evolutions, and finally detect it with certainty in Minkowski space-time. The critical step in quantum technology

Conceptual Challenges of Quantum Field Theory in Technology

ACKNOWLEDGEMENTS

REFERENCES

1. C.W. Misner, K.S. Thorne and J.A. Wheeler, W.H. Freeman and Company (1973) *Gravitation.* 1,1

2. R.M. Wald, Chicago University press (1984) *General Relativity.* 1, 1

3. S. Carroll, Addison Wesley (2004) *SPACETIME AND GEOMETRY An Introduction to General Relativity.*1, 1

4. J.D. Jackson, John Wily and Sons (1999) *Classical Electrodynamocs.* 1

5. G. Greenstein, A.G. Zajonc, Jones And Bartlett Publishers (2006) *The Quantum Challenge: Modern Research on the Foundations of Quantum Mechanics.* 1, 4.2

6. M.V. Takook, Razi university press (2017) *The physical view of the world.* 1, 2

7. A. Aspect, J. Dalibard and G. Roger, Phys. Rev. Lett. **49**, 1804 (1982) *Experimental test of Bell's inequalities using time-varying analyzers.* 2.2, 5.1

8. P. Grangier, G. Roger and A. Aspect, Europhysics Letters **1**, 173 (1986) *Experimental Evidence for a Photon Anticorrelation Effect on a Beam Splitter: A New Light on Single-Photon Interferences.* 2.2, 5.1

9. S.T. Ali, J.P. Antoine, J.P. Gazeau, Springer (2014) *Coherent States, Wavelets, and Their Generalizations.* 3.2,3.2

10. J.P. Gazeau, WILEY-VCH (2009) *Coherent States in Quantum Physics.* 3.2, 3.2

11. W. Kouchner, Springer (2006) *Solid-State Laser Engineering.* 3.2, 3.2

12. H. Yan, Marcel Dekker (2000) *Signal Processing for Magnetic Resonance: Imaging and Spectroscopy.* 3.2

13. T.M. Peters, J. Williams, Springer (1998) *The Fourier Transform in Biomedical Engineering.* 3.2

14. J. Aasi et al., Nature Photonics 7, 613 (2013) *Enhanced sensitivity of the LIGO gravitational wave detector by using squeezed states of light.* 3.2, 3.2

15. U.L. Andersen, Physica Scripta **91**, 053001 (2016) *30 years of squeezed light generation.* 3.2

16. H.J. Levinson, Society of Photo-Optical Instrumentation Engineers (2010) *Principles of Lithography.* 3.2

17. B. Yu, D.Z. Pan, Springer (2016) *Design for Manufacturability with Advanced Lithography.* 3.2

18. O. Gywat, H.J. Krenner, J. Berezovsky, WILEY-VCH (2010) *Spins in Optically Active Quantum Dots: Concepts and Methods.* 3.2, 5.2

19. L. Banyai, S.W. Koch, World Scientific Publishing (1993) *Semiconductor Quantum Dots.* 3.2, 5.2

20. A. Bienfait et al., Phys. Rev. X 7, 041011 (2017) *Magnetic Resonance with Squeezed Microwaves.* 3.2

21. K. Rottwitt, P. Tidemand-Lichtenberg, Taylor and Francis Group (2016) *Nonlinear Optics: Principles and Applications.* 3.2

22. G. Grynberg, A. Aspect, C. Fabre, Cambridge University Press (2010) *Introduction to Quantum Optics: From the Semi-classical Approach to Quantized Light.* 3.2

23. L. Dong, B. Samson; Taylor and Francis Group (2017) *Fiber Lasers: Basics, Technology and Applications.*3.2

Conceptual Challenges of Quantum Field Theory in Technology

24. L. Baulieu, J. Iliopoulos, R. Senior, Oxford University Press (2017) *Quantum field theory From Classical to Quantum Fields*. 4, 5.2

25. S. Weinberg, Cambridge University Press (1995) *The Quantum Theory of Fields*. 4.1

26. E. Brezin and S. Wadia, World Scientific (1993) *The large N expansion in quantum field theory and statistical physics*. 4.1, 5.2

27. E. Brezin, Cambridge University press (2010) *Introduction to statistical field theory*. 4.1, 5.2

28. C. Itzykson and J.B. Zuber, McGraw-Hill, New York (1980) *Quantum Field Theory*. 4.2

29. M, Nakahara, T. Ohmi, Taylor and Francis Group (2008) *Quantum Computing: From Linear Algebra to Physical Realizations*. 4.2, 5.3

30. M. Mano, Prentice Hall (1992) *Computer System Architecture*. 4.2

31. M.A. Nielsen, I.L. Chuang, Cambridge University Press (2010) *Quantum Computation and Quantum Information*. 4.2

32. A. Furusawa, P. Van Loock, WILEY-VCH (2011) *Quantum Teleportation and Entanglement: A Hybrid Approach to Optical Quantum Information Processing*. 4.2

33. P. Kok, B.W. Lovett, Cambridge University Press (2010) *Introduction to Optical Quantum Information Processing*. 4.2

34. J. Iliopoulos, Oxford University Press (2017) *The Origin of Mass Elementary Particles and Fundamental Symmetries*. 5

35. D.A. Neamen, McGraw-Hill (2003) *Semiconductor Physics and Devices: Basic Principles*. 5.1

36. M. Tinkham, McGraw-Hill (1996) *Introduction to superconductivity*. 5.1

37. Q. Bao, H.Y. Hoh, Y.Z. Pan, Stanford Publishing (2017) *Graphene: Photonics, Optoelectronics, and Plas- monics*. 5.1

38. J.E. Proctor, D. A. M. Armada, A. Vijayaraghavan, Taylor and Francis Group (2017) *An Introduction to Graphene and Carbon Nanotubes* . 5.1

39. J.M. Lourtioz, Springer (2008) *Photonic crystals towards nanoscale photonic devices*. 5.2

40. . Limpert et al., OPTICS EXPRESS **11**, 818 (2003) *High-power air-clad large-mode-area photonic crystal fiber laser*. 5.2

41. P. Harrison, JOHN WILEY and SONS (2005) *Quantum Wells Wires and dots: Theoretical and Computa- tional Physics of Semiconductor Nanostructures*. 5.2

42. H. Veendrick, Springer (2008) *Nanometer CMOS ICs: From basics to ASICs*. 5.2

43. D. Clein, Butterworth Heinemann (2000) *CMOS IC Layout: Concepts, Methodologie and Tools*. 5.2

44. A.C. Mahoney, J.I. Colless, L. Peeters, S.J. Pauka, E.J. Fox, X. Kou, L. Pan, K.L. Wang, D. Goldhaber- Gordon, D.J. Reilly, Nature Communication **18**, 1836 (2017) *Zero-field edge plasmons in a magnetic topo- logical insulator*. 5.2

45. S.A. Maier, Springer (2007) *Plasmonics: Fundamental and Applications*. 5.2

46. H. Weng, R. Yu, X. Hu, X. Dai, Z. Fang, Advances in Physics **64**, 227 (2015) *Quantum Anomalous Hall Effect and Related Topological Electronic States*. 5.2

47. C.X. Liu, S.C. Zhang, and X.L. Qi, Annu. Rev. Condens. Matter Phys. **7**, 301 (2016) *The quantum anomalous Hall effect Theory and Experiment*. 5.2

48. K.Y. Bliokh, D. Smirnova, and F. Nori, Science **348**, 1448 (2015) *Quantum spin Hall effect of light*. 5.2

49. D.G. Welsch, W. Vogel, T. Opatrny, Progress in Optics **XXXIX**, 63 (2009) *Homodyne Detection and Quantum State Reconstruction*. 5.3

50. H. Haffner et al., Nature **438**, 643 (2005) *Scalable multiparticle entanglement of trapped ions*. 5.3

51. D. Jaksch et al., Phys. Rev. Lett. **82**, 1975 (1999) *Entanglement of Atoms via Cold Controlled Collisions*. 5.3

Conceptual Challenges of Quantum Field Theory in Technology

London Journal Press Membership

For Authors, subscribers, Boards and organizations

London Journals Press membership is an elite community of scholars, researchers, scientists, professionals and institutions associated with all the major disciplines. London Journals Press memberships are for individuals, research institutions, and universities. Authors, subscribers, Editorial Board members, Advisory Board members, and organizations are all part of member network.

Read more and apply for membership here:
https://journalspress.com/journals/membership

For Authors

For Institutions

For Subscribers

Author Membership provide access to scientific innovation, next generation tools, access to conferences/seminars /symposiums/webinars, networking opportunities, and privileged benefits.
Authors may submit research manuscript or paper without being an existing member of LJP. Once a non-member author submits a research paper he/she becomes a part of "Provisional Author Membership".

Society flourish when two institutions come together." Organizations, research institutes, and universities can join LJP Subscription membership or privileged "Fellow Membership" membership facilitating researchers to publish their work with us, become peer reviewers and join us on Advisory Board.

Subscribe to distinguished STM (scientific, technical, and medical) publisher. Subscription membership is available for individuals universities and institutions (print & online). Subscribers can access journals from our libraries, published in different formats like Printed Hardcopy, Interactive PDFs, EPUBs, eBooks, indexable documents and the author managed dynamic live web page articles, LaTeX, PDFs etc.

JOURNAL AVAILABLE IN

PRINTED VERSION, INTERACTIVE PDFS, EPUBS, EBOOKS, INDEXABLE
DOCUMENTS AND THE AUTHOR MANAGED DYNAMIC LIVE WEB PAGE
ARTICLES, LATEX, PDFS, RESTRUCTURED TEXT, TEXTILE, HTML, DOCBOOK,
MEDIAWIKI MARKUP, TWIKI MARKUP, OPML, EMACS ORG-MODE & OTHER

SCAN TO KNOW MORE

support@journalspress.com
www.journalspress.com

*THIS JOURNAL SUPPORT AUGMENTED REALITY APPS AND SOFTWARES